Bijection between trees in Stanley character formula and factorizations of a cycle

by

Karolina Trokowska
Piotr Śniady

Max-Planck-Institut für Mathematik
Preprint Series 2022 (66)

Date of submission: October 12, 2022

Bijection between trees in Stanley character formula and factorizations of a cycle

by

Karolina Trokowska
Piotr Śniady

Max-Planck-Institut für Mathematik
Vivatsgasse 7
53111 Bonn
Germany

MPIM 22-66

BIJECTION BETWEEN TREES IN STANLEY CHARACTER FORMULA AND FACTORIZATIONS OF A CYCLE

KAROLINA TROKOWSKA AND PIOTR ŚNIADY

ABSTRACT. Stanley and Féray gave a formula for the irreducible character of the symmetric group related to a *multi-rectangular Young diagram*. This formula shows that the character is a polynomial in the multi-rectangular coordinates and gives an explicit combinatorial interpretation for its coefficients in terms of counting certain decorated maps (i.e., graphs drawn on surfaces). In the current paper we concentrate on the coefficients of the top-degree monomials in the Stanley character polynomial which corresponds to counting certain decorated plane trees. We give an explicit bijection between such trees and minimal factorizations of a cycle.

1. INTRODUCTION

1.1. **Normalized characters and Stanley polynomials.**

For a Young diagram λ with $N = |\lambda|$ boxes and a partition $\pi \vdash k$ we denote by

$$\operatorname{Ch}_\pi(\lambda) = \begin{cases} \underbrace{N(N-1)\cdots(N-k+1)}_{k \text{ factors}} \frac{\chi^\lambda\left(\pi\cup 1^{N-k}\right)}{\chi^\lambda\left(1^N\right)} & \text{for } k \leqslant N, \\ 0 & \text{otherwise} \end{cases}$$

the *normalized irreducible character of the symmetric group*, where $\chi^\lambda(\rho)$ denotes the value of the usual irreducible character of the symmetric group which corresponds to the Young diagram λ, evaluated on any permutation with the cycle decomposition given by the partition ρ. This choice of the normalization is very natural, see for example [IK99; Bia03]. One of the goals of the *asymptotic representation theory* is to understand the behavior of such normalized characters in the scaling when the partition π is fixed and the number of the boxes of the Young diagram λ tends to infinity.

2020 *Mathematics Subject Classification.* Primary: 05A19; Secondary: 05C05.

[0]An abridged, 12-page version of this paper was published in the proceedings of The 33rd International Conference on Formal Power Series and Algebraic Combinatorics (FPSAC 2021) [Woj21]; note that at the time of the FPSAC submission, the first named author of the current paper used a different surname.

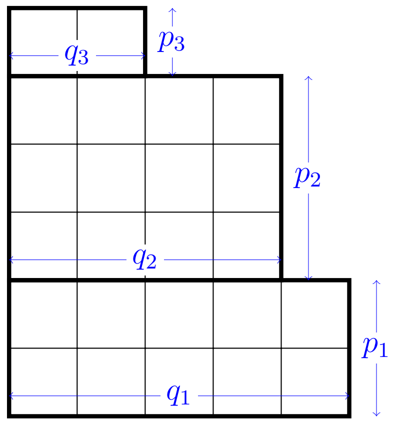

Figure 1. Multi-rectangular Young diagram $\mathbf{p} \times \mathbf{q} = (2,3,1) \times (5,4,2)$.

For a pair of sequences of non-negative integers $\mathbf{p} = (p_1, \dots, p_\ell)$ and $\mathbf{q} = (q_1, \dots, q_\ell)$ such that $q_1 \geqslant \cdots \geqslant q_\ell$ we consider the *multi-rectangular Young diagram* $\mathbf{p} \times \mathbf{q}$, see Figure 1. Stanley [Sta03; Sta06] initiated investigation of the normalized characters evaluated on such multi-rectangular Young diagrams and proved that

$$(\mathbf{p}, \mathbf{q}) \mapsto \operatorname{Ch}_\pi (\mathbf{p} \times \mathbf{q}) \tag{1}$$

is a polynomial (called now *the Stanley character polynomial*) in the variables $p_1, \dots, p_\ell, q_1, \dots, q_\ell$. He also gave a conjectural formula (proved later for the top-degree part by Rattan [Rat08] and in the general case by Féray [Fér10]) which gives a combinatorial interpretation to the coefficients of this polynomial in terms of certain *maps* (i.e., graphs drawn on surfaces). Stanley also explained how investigation of its coefficients might shed some light on the *Kerov positivity conjecture*, see [Śni16] for more context.

Despite recent progress in this field (for the proof of the Kerov positivity conjecture see [Fér09; DFŚ10]) there are several other positivity conjectures related to the normalized characters Ch_π that remain open (see [GR07, Conjecture 2.4] and [Las08]) and which suggest the existence of some additional hidden combinatorial structures behind such characters. We expect that such positivity problems are more amenable to bijective methods (such as the ones from [Cha09]) and the current article is the first step in this direction.

We will concentrate on the special case when the partition $\pi = (k)$ consists of a single part. In this case the degree of the Stanley polynomial (1) turns out to be equal to $k+1$. We will also concentrate on the combinatorial interpretation of the coefficients of the Stanley polynomial (1) standing at monomials of this maximal degree $k+1$; they turn out to be related to maps of genus zero, i.e., *plane trees*. Nevertheless, the methods which we present in the current paper for this special case are applicable in much bigger generality and in a forthcoming paper we discuss the applications to maps with higher genera.

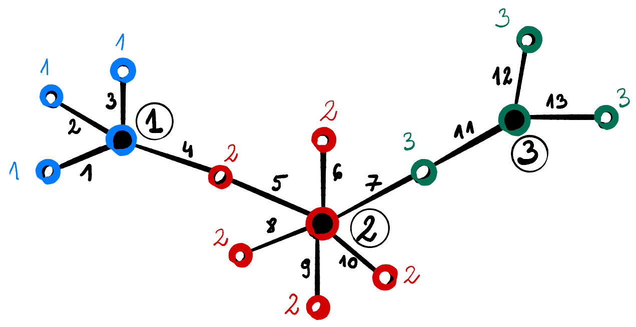

Figure 2. An example of a Stanley tree of type $(3,5,3)$. The circled numbers indicate the labels of the black vertices. The black numbers indicate the labels of the edges. The colors (blue for 1, red for 2, green for 3) indicate the values of the function f on white vertices.

1.2. **Stanley trees.** Let T be a *bicolored* plane tree, i.e., a plane tree with each vertex painted black or white and with edges connecting the vertices of opposite colors. We assume that the tree has k edges labeled with the numbers $1,\dots,k$. We also assume that it has n black vertices labeled with the numbers $1,\dots,n$. The white vertices are not labeled. Being *a plane tree* means that the set of edges surrounding any given vertex is equipped with a cyclic order related to visiting the edges in the counterclockwise order. In our context the structure of the plane tree can be encoded by a pair of permutations (σ_1,σ_2) with $\sigma_1,\sigma_2 \in \mathfrak{S}_k$ such that the cycles of σ_1 (respectively, the cycles of σ_2) correspond to labels of the edges surrounding white (respectively, black) vertices. We define the function f which to each white vertex associates the maximum of the labels of its black neighbors. We will say that T is a *Stanley tree of type*

$$(b_1,\dots,b_n) := \Big(\big|f^{-1}(1)\big|,\dots,\big|f^{-1}(n)\big| \Big);$$

in other words the type gives the information about the number of the white vertices for which the function f takes a specified value. Figure 2 gives an example of a Stanley tree of type $(3,5,3)$.

Since for a tree the total number of the black and the white vertices is equal to the number of the edges plus 1, it follows that

$$b_1+\cdots+b_n+n = k+1. \tag{2}$$

Note that the definition of the Stanley tree of a given type depends implicitly on the value of k; in the following we will always assume that k is given by (2).

By $\mathcal{T}_{b_1,\dots,b_n}$ we denote the set of Stanley trees of a specific type $(b_1,\dots,b_n)$.

1.3. **Coefficients of the top-degree $\mathbf{p}$-square-free monomials.** It turns out that in the analysis of the Stanley polynomials it is enough to restrict attention to *the* $\mathbf{p}$*-square-free* *monomials*, i.e., the monomials of the form

$$p_1 \cdots p_n q_1^{b_1} \cdots q_n^{b_n} \tag{3}$$

with integers $b_1, \dots, b_n \geqslant 0$, see [DFŚ10, Section 4] and [Śni16] for a short overview. The following lemma is a reformulation of a result of Rattan [Rat08] and gives a combinatorial interpretation to the coefficients standing at these $\mathbf{p}$-square-free monomials which are of top-degree.

Lemma 1.1. *For all integers $b_1, \dots, b_n \geqslant 0$ such that*

$$b_1 + \cdots + b_n + n = k + 1 \tag{4}$$

the $\mathbf{p}$-square-free coefficient of the Stanley character polynomial is given by

$$\left[p_1 \cdots p_n q_1^{b_1} \cdots q_n^{b_n}\right] \operatorname{Ch}_k \left(\mathbf{p} \times \mathbf{q}\right) = \pm \frac{1}{(k-1)!} \left|\mathcal{T}_{b_1,\dots,b_n}\right|. \tag{5}$$

In order to be concise we will not discuss the sign on the right-hand side. The above lemma is a special case of a general formula conjectured by Stanley [Sta06, Conjecture 3] and proved by Féray [Fér10] and therefore we refer to it as the Stanley–Féray character formula. This general formula is applicable also when the assumption (4) is not fulfilled; in this case on the right-hand side of (5) the Stanley trees should be replaced by *unicellular maps* with some additional decorations, see Section 1.5.1 for more details.

There is another way of calculating the coefficient on the left-hand side of (5); we shall review it in the following. The homogeneous part of degree $k+1$ of the multivariate polynomial $\operatorname{Ch}_k \left(\mathbf{p} \times \mathbf{q}\right)$ (i.e., its homogeneous part of the top degree) is called *the free cumulant* and is denoted by $R_{k+1}\left(\mathbf{p} \times \mathbf{q}\right)$. Free cumulants were first defined in the context of Voiculescu's free probability theory and the random matrix theory (see [DFŚ10, Sections 1.3 and 3.4] for references); in the context of the representation theory of the symmetric groups they were introduced in the fundamental work of Biane [Bia98]. From the defining property of the free cumulant it follows that

$$\left[p_1 \cdots p_n q_1^{b_1} \cdots q_n^{b_n}\right] \operatorname{Ch}_k \left(\mathbf{p} \times \mathbf{q}\right) = \left[p_1 \cdots p_n q_1^{b_1} \cdots q_n^{b_n}\right] R_{k+1}\left(\mathbf{p} \times \mathbf{q}\right), \tag{6}$$

provided that (4) holds true.

Dołęga, Féray and the second named author [DFŚ10, Section 3.2] introduced another convenient family $S_2, S_3, \dots$ of functions on the set of Young diagrams, which has the property that for any *strictly positive* exponents $b_1, \dots, b_n \geqslant 1$ the coefficient of the corresponding $\mathbf{p}$-square-free monomial (3) in any finite product

$$S_2^{\alpha_2} S_3^{\alpha_3} \cdots = \left[S_2\left(\mathbf{p} \times \mathbf{q}\right)\right]^{\alpha_2} \left[S_3\left(\mathbf{p} \times \mathbf{q}\right)\right]^{\alpha_3} \cdots$$

(for any sequence of integers $\alpha_2, \alpha_3, \dots \geqslant 0$ such that only finitely many of its entries are non-zero) takes a particularly simple form, cf. [DFŚ10, Theorem 4.2]. On the other hand, the free cumulant R_{k+1} can be written as an explicit polynomial in the functions $S_2, S_3, \dots$, cf. [DFŚ10, Proposition 2.2]. By combining these two results it follows that for any integers $b_1, \dots, b_n \geqslant 1$ such that (4) holds true, the right-hand side of (6) is equal to

$$\left[p_1 \cdots p_n q_1^{b_1} \cdots q_n^{b_n}\right] R_{k+1}(\mathbf{p} \times \mathbf{q}) = (-k)^{n-1}. \tag{7}$$

By combining Equations (5)–(7) we obtain the following result.

Corollary 1.2. *For any integers* $b_1, \dots, b_n \geqslant 1$ *such that* (4) *holds true, the number of the Stanley trees of type* $(b_1, \dots, b_n)$ *is equal to*

$$\left|\mathcal{T}_{b_1,\dots,b_n}\right| = (k-1)!\, k^{n-1}. \tag{8}$$

Remark 1.3. The assumption that the $b_1, \dots, b_n$ are *strictly* positive cannot be weakened; if some of the entries of the sequence $b_1, \dots, b_n$ are equal to zero then the number of the Stanley trees of type $(b_1, \dots, b_n)$ takes a more complicated form which can be extracted by an application of [DFŚ10, Lemma 4.5].

The above sketch of the proof of Corollary 1.2 has a disadvantage of being purely algebraic. The main result of the current paper (see Theorem 2.1 below) is its new, bijective proof. As the first step in this direction we will look for some natural class of combinatorial objects the cardinality of which is given by the right-hand side of (8).

1.4. Minimal factorizations of long cycles.

We fix an integer $k \geqslant 1$ and denote by $\mathfrak{S}_k$ the corresponding symmetric group. We say that a permutation $\pi \in \mathfrak{S}_k$ is a *cycle of length* ℓ if it is of the form $\pi = (x_1, \dots, x_\ell)$.

Let $a_1, \dots, a_n \geqslant 2$ be integers. We say that a tuple $(\sigma_1, \dots, \sigma_n)$ is a *factorization of a long cycle of type* $(a_1, \dots, a_n)$ if $\sigma_1, \dots, \sigma_n \in \mathfrak{S}_k$ are such that the product $\sigma_1 \cdots \sigma_n$ is a cycle of length k and σ_i is a cycle of length a_i for each choice of $i \in \{1, \dots, n\}$. In the current paper we concentrate on *minimal factorizations* which correspond to the special case when

$$\sum_{i=1}^{n} (a_i - 1) = k - 1. \tag{9}$$

By $\mathcal{C}_{a_1,\dots,a_n}$ we denote the set of such minimal factorizations of a long cycle of type $(a_1, \dots, a_n)$.

Biane [Bia96] extended a previous result of Dénes [Dén59] and proved that the number of minimal factorizations $\sigma = \sigma_1 \dots \sigma_n$ of a *fixed* cycle σ of length k into a product of cycles of lengths $a_1, \dots, a_n$ for which (9) is fulfilled, is equal to k^{n-1}. Since in the symmetric group $\mathfrak{S}_k$ there are $(k-1)!$ such cycles σ of length k, it follows that the number of the minimal factorizations of a long cycle of type $(a_1, \dots, a_n)$ is equal to

$$\left|\mathcal{C}_{a_1,\dots,a_n}\right| = (k-1)!\, k^{n-1} \tag{10}$$

and therefore coincides with the right-hand side of (8). Our new proof of Corollary 1.2 will be based on an explicit bijection between the set $\mathcal{T}_{b_1,\dots,b_n}$ of Stanley trees of some specified type and the set $\mathcal{C}_{a_1,\dots,a_n}$ of minimal factorizations of a long cycle of some specified type, see Theorem 2.1 for more details.

1.5. **Outlook: permutations, plane trees, maps.**

For simplicity, in the current paper we consider only *the first-order* asymptotics of the character (1) of the symmetric group on a cycle $\pi = (k)$, which corresponds to the coefficients of the Stanley polynomial (5) appearing at the top-degree monomials (4). In the light of the aforementioned open problems which concern the fine structure of the symmetric group characters Ch_k evaluated on a cycle (see [GR07, Conjecture 2.4] and [Las08]) it would be interesting to extend the results of the current paper to the coefficients of *general* $\mathbf{p}$-square-free monomials of the Stanley character polynomial. We will keep this wider perspective in mind in what follows.

Each of the two sets $\mathcal{T}_{b_1,\dots,b_n}$ and $\mathcal{C}_{a_1,\dots,a_n}$ which appear in our main bijection has an algebraic facet and a geometric facet. In the following we will revisit the links between these facets. These geometric facets will be essential for the bijection which is the main result of the current paper.

1.5.1. *Stanley trees, revisited.*

The general form of the Stanley–Féray character formula (see [Sta06, Conjecture 3] and Féray [Fér10]) gives an explicit combinatorial interpretation to the coefficient of an *arbitrary* monomial in the Stanley polynomial $\operatorname{Ch}_k\big(\mathbf{p}\times\mathbf{q}\big)$, nevertheless it seems that in applications only $\mathbf{p}$-square-free monomials are really useful, see [DFŚ10, Section 4] and [Śni16]. It turns out that in general the coefficient

$$[p_1\cdots p_n q_1^{b_1}\cdots q_n^{b_n}]\operatorname{Ch}_k\big(\mathbf{p}\times\mathbf{q}\big) \tag{11}$$

is equal (up to the $\pm$ sign) to the number of triples (σ_1,σ_2,f_2) such that:

- $\sigma_1,\sigma_2\in\mathfrak{S}_k$ are permutations with the property that their product
$$\sigma_1\sigma_2=(1,2,\dots,k)$$
is a specific cycle of length k;
- f_2 is a bijection between the set of cycles of the permutation σ_2 and the set $\{1,\dots,n\}$ (we can think that f_2 is a *labeling* of the cycles of σ_2);
- we define the function f_1 on the set of cycles of the permutation σ_1 by setting
$$f_1(c_1)=\max\big\{f_2(c_2) : c_2 \text{ is a cycle of } \sigma_2 \text{ such that the cycles } c_1 \text{ and } c_2 \text{ are \emph{not} disjoint}\big\} \quad \text{if } c_1 \text{ is a cycle of } \sigma_1;$$
we require that for each $i\in\{1,\dots,n\}$ the cardinality of its preimage is given by the appropriate exponent of the variable q_i in the monomial:
$$\big|f_1^{-1}(i)\big| = b_i.$$

To this algebraic object $(\sigma_1, \sigma_2, f_2)$ one can associate a geometric counterpart, which is a *bicolored map*. More specifically, it is a graph drawn on an oriented surface, with the edges labeled with the elements of the set $\{1, \dots, k\}$. Each white vertex (respectively, each black vertex) corresponds to some cycle of the permutation σ_1 (respectively, to some cycle of the permutation σ_2) so that the counterclockwise cyclic order of the edges around the vertex coincides with the cyclic order of the elements of the set $\{1, \dots, k\}$ which are permuted by the cycle, see [Śni13, Section 6.4].

We assume that the surface on which the graph is drawn is *minimal* which means that after cutting the surface along the edges, each connected component is homeomorphic to a disc; we call such connected components *faces* of the map. The product $\sigma_1\sigma_2 = (1, 2, \dots, k)$ consists of a single cycle which geometrically means that our map has exactly one face; in other words it is *unicellular*.

The bijection f_2 geometrically means that the black vertices of our map are labeled by the elements of the set $\{1, \dots, n\}$. Using such a geometric viewpoint, f_1 becomes a function on the set of white vertices which to a given white vertex associates the maximum of the labels (given by f_2) of its neighboring black vertices.

By counting the white and the black vertices it follows that the total number of the vertices is equal to

$$b_1 + \cdots + b_n + n.$$

A simple argument based on the Euler characteristic shows that for a unicellular map this number of vertices is bounded from above by $k + 1$ (which is the number of the edges plus one) and the inequality becomes saturated (i.e., the equality (4) holds true) if and only if the surface has genus zero, i.e., it is homeomorphic to a sphere.

In the following we consider the case when (4) indeed holds true. It is conceptually simpler to consider such a map drawn on the sphere as drawn on the plane; being unicellular corresponds to the map being a tree. It follows that in this case the geometric object associated above to the triple $(\sigma_1, \sigma_2, f_2)$ which contributes to the coefficient (11) coincides with the Stanley tree of type $(b_1, \dots, b_n)$.

The above discussion motivates the notion of the Stanley trees and shows which more general geometric objects should be investigated in order to study more refined asymptotics of the characters of the symmetric groups.

1.5.2. *Minimal factorizations.* The geometric object which can be associated to a minimal factorization $\sigma_1, \dots, \sigma_n \in \mathfrak{S}_k$ of a long cycle of type $(a_1, \dots, a_n)$ is a graph with k white vertices (labeled with the elements of the set $\{1, \dots, k\}$) and n black vertices (labeled with the elements of the set $\{1, \dots, n\}$). We connect the black vertex i with the white vertices $\sigma_{i,1}, \dots, \sigma_{i,a_i}$ which correspond to the elements of the cycle $\sigma_i = (\sigma_{i,1}, \dots, \sigma_{i,a_i})$. This graph is clearly connected, it has $k + n$ vertices and it has $a_1 + \cdots + a_n$ edges; from the minimality assumption (9) it follows that the graph is, in fact, a tree. We may encode the cycles $\sigma_1, \dots, \sigma_n$ by drawing the tree on the plane in such a way that the counterclockwise order of the white vertices surrounding a given black vertex i corresponds to the cycle σ_i. On the other hand, we have a freedom of choosing the cyclic order of the edges around the white vertices. In this way a minimal factorization of a long cycle can be encoded by a plane tree with labeled white vertices and labeled black vertices.

1.6. **Overview of the paper.**

In Section 2 we state our main result (Theorem 2.1) about existence of a bijection between certain sets of minimal factorizations and Stanley trees; the bijection itself is constructed in Sections 2.1, 2.2, 2.5 and 2.7. It is quite surprising that a bare-boned description of the bijection (without the proof of its correctness) is quite short, nevertheless this algorithm creates a quite complex dynamics, as can be seen by the length of the description of the inverse map. Additionally, in Sections 2.6 and 2.8 we prove that this algorithm is well defined.

As the first step towards the proof of Theorem 2.1, in Section 3 we show Proposition 3.2 which states that the output of our algorithm indeed is a Stanley tree of a specific type.

Section 4 contains an alternative description of the bijection.

In Section 5 we construct the inverse map.

Finally, in Section 6 we complete the proof of Theorem 2.1.

2. The main result: bijection between Stanley trees and minimal factorizations of long cycles

The following is the main result of the current paper.

Theorem 2.1. *Let $n \geqslant 2$ and $b_1, \dots, b_n \geqslant 1$ be integers. We define the integers $a_1, \dots, a_n$ by*

$$a_i = \begin{cases} b_i + 1 & \text{if } i \in \{1, n\}, \\ b_i + 2 & \text{otherwise}. \end{cases} \tag{12}$$

Then the algorithm $\mathcal{A}$ presented below gives a bijection between the set $\mathcal{C}_{a_1,\dots,a_n}$ of minimal factorizations (see Section 1.4) and the set $\mathcal{T}_{b_1,\dots,b_n}$ of Stanley trees (see Section 1.2).

Note that both the notion of a Stanley tree as well as the notion of the minimal factorization implicitly depend on the value of k given, respectively, by (2) and (9). In our context, when (12) holds true, these two values of k coincide.

2.1. **The first step of the algorithm $\mathcal{A}$: from a factorization to a tree with repeated edge labels.**

In the first step of our algorithm $\mathcal{A}$ to a given minimal factorization $(\sigma_1, \dots, \sigma_n) \in \mathcal{C}_{a_1,\dots,a_n}$ we will associate a bicolored plane tree T_1 with labeled black vertices and labeled edges. The remaining part of the current section is devoted to the details of this construction.

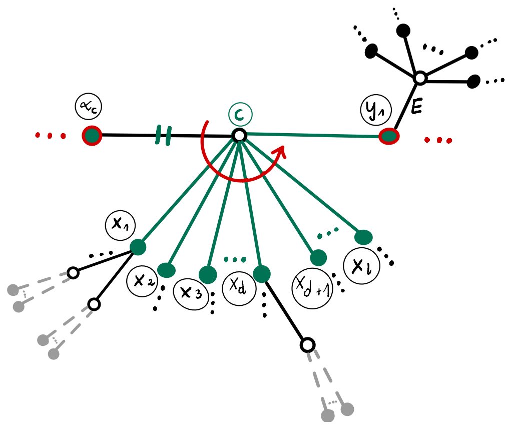

Figure 3. The structure of a white spine vertex c in the plane tree T_0. The labels of the black spine vertices $\alpha_c, y_1 \in \{1, \dots, n\}$ fulfill $\alpha_c < y_1$.

2.1.1. *The tree* T_0. Just like in Section 1.5.2 we start by creating a graph T_0 with n black vertices labeled $1, \dots, n$ and with k white vertices labeled $1, \dots, k$, where k is given by (9). Each black vertex i corresponds to the cycle $\sigma_i = (\sigma_{i,1}, \dots, \sigma_{i,a_i})$ and so we connect the black vertex i with the white vertices $\sigma_{i,1}, \dots, \sigma_{i,a_i}$. By the same argument as in Section 1.5.2 this graph is, in fact, a tree.

In order to give this tree the structure of a *plane tree* we need to specify the cyclic order of the edges around each vertex. Just like in Section 1.5.2 we declare that going counterclockwise around the black vertex i the cyclic order of the labels of the white neighbors should correspond to the cyclic order $\sigma_{i,1}, \dots, \sigma_{i,a_i}$. The cyclic order around the white vertices is more involved and we present it in the following.

The path between the two black vertices with the labels 1 and n will be called *the spine*; on Figure 4a it is drawn as the horizontal red path. There will be two separate rules which determine the cyclic order of the edges around a given white vertex, depending whether the vertex belongs to the spine or not.

For each white vertex which is *not* on the spine we declare that going counterclockwise around it, the labels of its black neighbors should be arranged in the increasing way (for example, the neighbors of the white vertex 6 on Figure 4a listed in the counterclockwise order are $3, 4, 6$).

For each white vertex c which belongs to the spine there are exactly two black neighbors which belong to the spine; we denote their labels by α_c and y_1 with $\alpha_c < y_1$, see Figure 3. Going counterclockwise around c, all non-spine edges should be inserted after α_c and before y_1. Their order is determined by the requirement that—after neglecting the

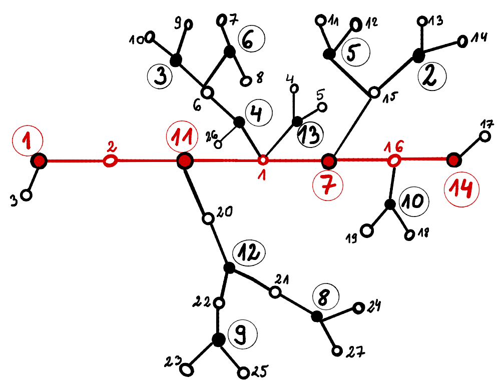
(a)

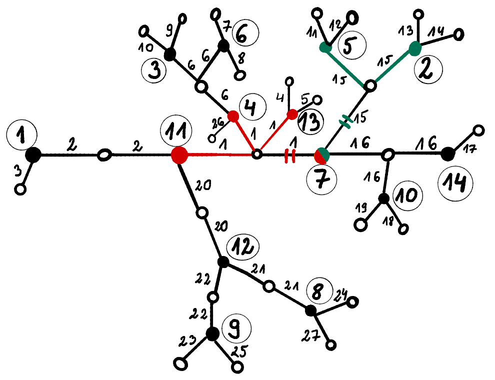
(b)

Figure 4. (a) The output T_0 of the first step of the algorithm $\mathcal{A}$ applied to the minimal factorization (13). The spine is the horizontal red path between the vertices 1 and 14. (b) The tree T_1 with some sample clusters highlighted. The red color indicates the cluster 1, while the green indicates the cluster 15. The double transverse lines identify the roots of the respective clusters.

vertex y_1—the cyclic counterclockwise order of the remaining vertices should be increasing. For example, for the white vertex 1 on Figure 4a we have $\alpha_1 = 7$, $y_1 = 11$ and the counterclockwise cyclic order of the non-y_1 black neighbors is $4, 7, 13$.

For example, Figure 4a gives the tree T_0 which corresponds to

$$n = 14, \quad k = 27, \quad a_1 = a_{14} = 2, \quad a_2 = \cdots = a_{13} = 3$$

and the minimal factorization $(\sigma_1, \dots, \sigma_{14}) \in \mathcal{C}_{2,3^{12},2}$

$$\begin{aligned} (13) \quad & \sigma_1 = (2,3), \quad \sigma_2 = (13,15,14), \quad \sigma_3 = (6,9,10), \quad \sigma_4 = (1,6,26), \\ & \sigma_5 = (11,15,12), \quad \sigma_6 = (6,8,7), \quad \sigma_7 = (1,16,15) \quad \sigma_8 = (21,27,24), \\ & \sigma_9 = (22,23,25), \quad \sigma_{10} = (16,19,18), \quad \sigma_{11} = (2,20,1), \\ & \sigma_{12} = (20,22,21), \quad \sigma_{13} = (1,5,4), \quad \sigma_{14} = (16,17). \end{aligned}$$

We denote by T_1 the tree T_0 in which each edge is labeled by its white endpoint and then all labels of the white vertices are removed, see Figure 4b. The tree T_1 is the output of the first step of the algorithm $\mathcal{A}$.

2.1.2. *Information about the initial tree T_1.* In the current section we will define certain sets and functions which describe the shape of the initial tree T_1. In the language of programmers: we will create variables B_c, α_c, $\mathcal{B}$, and $\mathfrak{C}$ which will not change their values during the execution of the algorithm $\mathcal{A}$.

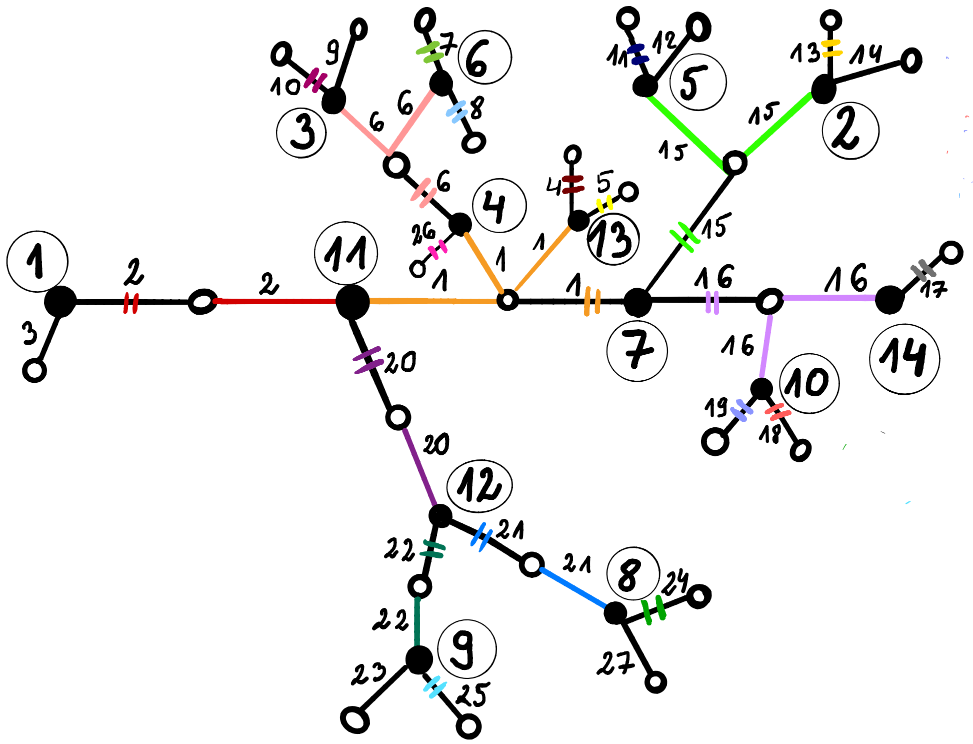

Figure 5. The tree T_1 which is the starting point of the second step of the algorithm $\mathcal{A}$. Essentially this is an enlarged version of Figure 4b with some additional highlights. For the sake of clarity we paint the non-root edges of each cluster in one color, while the root edge is marked with two transverse lines of the same color.

For $c \in \{1, \dots, k\}$ by *the cluster* c we mean the set of edges which carry the label c, together with their black endpoints. We will also say that c is the label of this cluster. All edges in a given cluster have the same white endpoint; this property will be preserved by the action of our algorithm. This common white vertex will be called *the center* of the cluster. For example, in Figure 4b the cluster 1 is drawn in red, while the cluster 15 is drawn in green.

A cluster is called a *spine cluster* if it contains exactly two black spine vertices. The set of labels of such spine clusters will be denoted by $\mathfrak{C} \subseteq \{1, \dots, k\}$.

We orient the non-spine edges of the tree so that the arrows point towards the spine. The *root of a non-spine cluster* is defined as the unique edge outgoing from the center. The *root of a spine cluster* is defined as the edge with the smallest label of the black endpoint among the two spine edges in the cluster; with the notations of Figure 3 it is the edge between the vertices c and α_c. For example, in Figure 5 the root of a cluster is marked with two transverse lines. Heuristically, our strategy will be to keep removing the edges from the cluster; the root is the unique cluster edge which will remain.

The black end of the root of a cluster $c \in \{1, \dots, k\}$ in the tree T_1 will be called *the anchor* of the cluster c and will be denoted by $\alpha_c \in \{1, \dots, n\}$. By definition, the anchor of a cluster will not change during the execution of the algorithm. We denote by $B_c \subseteq \{1, \dots, n\}$ the set of labels of the black vertices in the cluster c in the tree T_1. The notion of the root will not be used in the description of the algorithm $\mathcal{A}$, nevertheless it will be a convenient tool for proving later its correctness.

By $\mathcal{B} \subseteq \{1, \dots, n\}$ we denote the set of the labels of black spine vertices.

For the example from Figure 4b we have:

$$\begin{aligned} &\mathcal{B} = \{1,7,11,14\}, \quad \mathfrak{C} = \{1,2,16\}, \\ &\quad B_1 = \{4,7,11,13\}, \quad B_2 = \{1,11\}, \quad B_6 = \{3,4,6\}, \quad B_{15} = \{2,5,7\}, \\ &\qquad B_{16} = \{7,10,14\}, \quad B_{20} = \{11,12\}, \quad B_{21} = \{8,12\}, \quad B_{22} = \{9,12\}, \\ &\alpha_1 = 7, \quad \alpha_2 = 1, \quad \alpha_6 = 4, \quad \alpha_{15} = 7, \\ &\qquad\qquad \alpha_{16} = 7, \quad \alpha_{20} = 11, \quad \alpha_{21} = 12, \quad \alpha_{22} = 12. \end{aligned} \tag{14}$$

We did not list the values of B_i and α_i for white vertices i which are non-spine leaves because these values will not be used by our algorithm.

A cluster is called a *leaf* if it contains exactly one edge. For example, in Figure 4b the cluster 10 is a leaf.

Recall that we orient the non-spine edges of the tree so that the arrows point towards the spine. The set of non-spine clusters is partially ordered by the orientations of the edges as follows: a cluster c_1 is a predecessor of a cluster c_2 if the path from the spine to the center of the cluster c_2 passes through the center of the cluster c_1. This partial order can be extended to a linear order (not necessarily in a unique way). Let Σ be the sequence of the clusters which are non-spine and non-leaf, arranged according to this linear order. For example, for the tree T_1 shown on Figure 4a we can choose $\Sigma = (6, 15, 20, 21, 22)$.

In the plane tree T_1 we can divide the set of white non-spine vertices (respectively, the set of non-spine clusters) into the set of *leftist* vertices and the set of *non-leftist* vertices (respectively, clusters). A white non-spine vertex (respectively, a non-spine cluster) is called *leftist* in the tree T_1 if it is the leftmost child of its parent. For example, for the tree T_1 shown on Figure 6, white leftist vertices are drawn as thick green empty circles.

2.2. **The second step of the algorithm $\mathcal{A}$: from a tree with repeated edge labels to a tree with unique edge labels.**

The starting point of the second step of our algorithm $\mathcal{A}$ is the bicolored plane tree T_1 with black vertices labeled $1, \dots, n$ and with edges labeled with

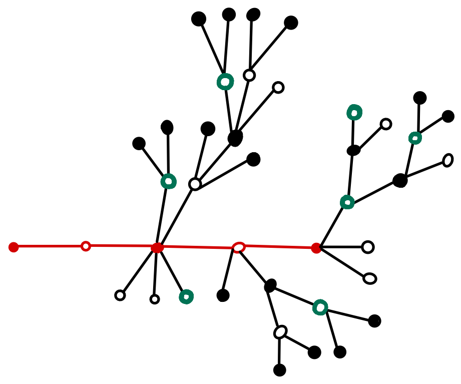

Figure 6. The tree T_1 shown without the labels. The red edges indicate the spine. The thick green empty circles indicate white leftist vertices.

the numbers $1, \dots, k$; note that the edge labels are repeated. Our goal in this second step of the algorithm is to transform the tree so that the edge labels are not repeated.

We declare that at the beginning all clusters of the tree T_1 are *untouched*. Also, each non-spine black vertex is declared to be *untouched* while each black spine vertex is declared to be *touched*.

The second step of the algorithm will consist of two parts: firstly we apply *the spine treatment* (Section 2.5), then we apply *the rib treatment* (Section 2.7). In fact, these two parts are very similar: each of them consists of an external loop which has a nested internal loop; one could merge these two parts and regard them as an instance of a single external loop which treats the spine vertices and the nib-spine vertices in a slightly different way.

During the action of the forthcoming algorithm some edges will be removed from each cluster. The root of the cluster may change during the execution of the algorithm. On the positive side, the following invariant guarantees that some properties of a cluster will persist (the proof is postponed to Proposition 2.5 and Proposition 2.7).

Invariant 2.2. *At each step of the algorithm and for each cluster c the following properties hold true:*

- *(I1) the edges of the cluster c have a common white endpoint (called, as before,* the center *of the cluster),*
- *(I2) the anchor of c is a black vertex which is connected by an edge with the center of c,*
- *(I3) the root of c is one of the edges which form the cluster c,*
- *(I4) if the black endpoint of the root of c is not equal to the anchor α_c then this black endpoint is touched.*

Be advised that distinct clusters might at later stages of the algorithm share the same center. Also, the anchor of a given cluster might no longer belong to the cluster.

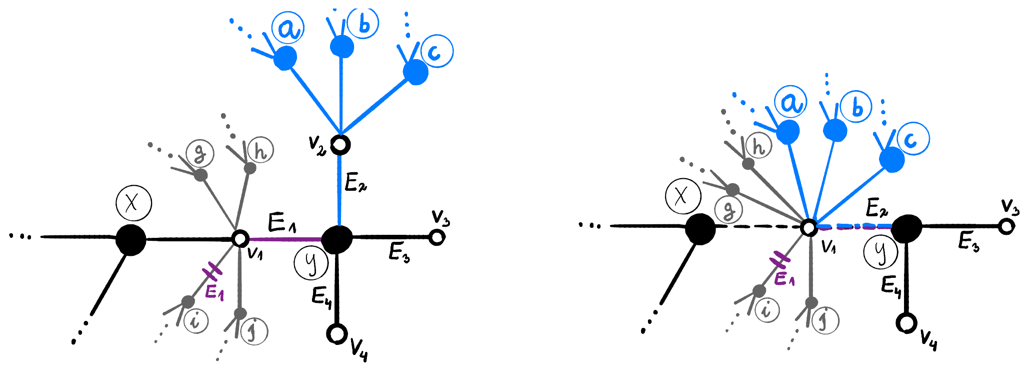

(a) (b)

Figure 7. (a) The initial configuration of the tree. (b) The output of $\mathbb{B}_{x,y}$.

The algorithm will be described in terms of two operations, called *bend* and *jump*; we present them in the following. Each of them decreases the number of the white vertices by 1, as well as decreases the number of edges by 1.

2.3. The building blocks of the second step: bend $\mathbb{B}_{x,y}$.

2.3.1. *Assumptions about the input of* $\mathbb{B}_{x,y}$. We list below the assumptions about the input of the operation *bend*. We also introduce some notations.

(B1) The operation $\mathbb{B}_{x,y}$ takes as an input a bicolored tree T which is assumed to be as in Invariant 2.2, together with a choice of two distinct black vertices x, y. We assume that there is a cluster E_1 such that x is the anchor of E_1 and y belongs to E_1, see Figure 7a. We denote the center of E_1 by v_1.

(B2) We denote by i the black endpoint of the root of the cluster E_1. We assume that $i \neq y$.

(B3) We also assume that the black vertex y has degree $d \geqslant 2$; we denote the edges around the vertex y by $E_1, \dots, E_d$ (going clockwise, starting from the edge E_1 between v_1 and y). We denote the white endpoint of the edge E_i by v_i.

2.3.2. *The output of* $\mathbb{B}_{x,y}$. The bend operation can be thought of as a counterclockwise rotation of the edge E_2 around the vertex y so that it is merged with the edge E_1; a more formal description of the output of $\mathbb{B}_{x,y}$ is given as follows.

We remove the edge between the vertices y and v_2. The label of the edge between v_1 and y is changed to E_2. If the removed edge was the root of the cluster E_2, the aforementioned edge between v_1 and y becomes the new root of the cluster E_2.

Then we merge the vertex v_2 with the vertex v_1 in such a way that going clockwise around v_1 the newly attached edges are immediately before the edge E_2 (these edges are marked blue on Figure 7).

From the following on we declare that the cluster E_1 is *touched* and also the black vertex y is *touched*. It is easy to check that the output tree still fulfills the properties from Invariant 2.2.

We will say that some operation on the tree *separates the root and the anchor in a cluster* c if (i) *before* this operation was applied the anchor of c was the black endpoint of the root of c, and (ii) *after* this operation is performed this is no longer the case. It is easy to check that the following simple lemma holds true.

Lemma 2.3. *The bend operation does not separate the root and the anchor in any cluster.*

2.4. **The building blocks of the second step: jump $\mathbb{J}_{x,y}$.**

2.4.1. *Assumptions about the input of* $\mathbb{J}_{x,y}$. We list below the assumptions about the input of the operation *jump*. We also introduce some notations.

(J1) The operation $\mathbb{J}_{x,y}$ takes as an input a bicolored tree T which is assumed to be as in Invariant 2.2, together with a choice of two black vertices x, y. We assume that there is a cluster E_1 such that x is the anchor of E_1 and y belongs to E_1, see Figures 8a and 9a. We denote by v_1 the center of the cluster E_1. We also assume that the labels of the vertices $x, y \in \{1, \dots, n\}$ fulfill $x < y$.

(J2) We denote by j the black neighbor of v_1 which—going clockwise around the vertex v_1—is immediately after y (note that it might happen that $j = x$, see Figure 9a). We assume that j is the black endpoint of the root of the cluster E_1, see Figures 8a and 9a.

(J3) We also assume that the black vertex y has degree $d \geqslant 3$; we denote the edges around the vertex y by $E_1, \dots, E_d$ (going clockwise, starting from the edge E_1). For $i \in \{1, \dots, d\}$ we denote the white endpoint of the edge E_i by v_i.

(J4) We assume that the vertex x is touched.

2.4.2. *The output of* $\mathbb{J}_{x,y}$. The output of $\mathbb{J}_{x,y}$ is defined as follows. We remove the three edges connecting y with the three vertices v_1, v_2, v_3. We create a new white vertex denoted w; this vertex is said to be *artificial*; we will use this notion later in the analysis of the algorithm.

We connect w to the vertex j by a new edge which we label E_2; more specifically, going clockwise around j the newly created edge E_2 is immediately after the edge E_1. This newly created edge replaces the removed edge between y and v_2, so if this removed edge was the root of the cluster E_2, we declare that the new edge E_2 becomes now the new root of the cluster E_2.

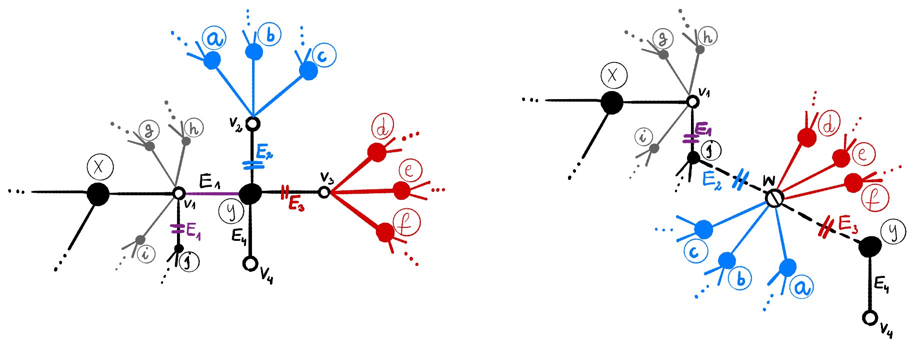

(a) (b)

Figure 8. (a) The initial configuration of the tree. (b) The output of $\mathbb{J}_{x,y}$.

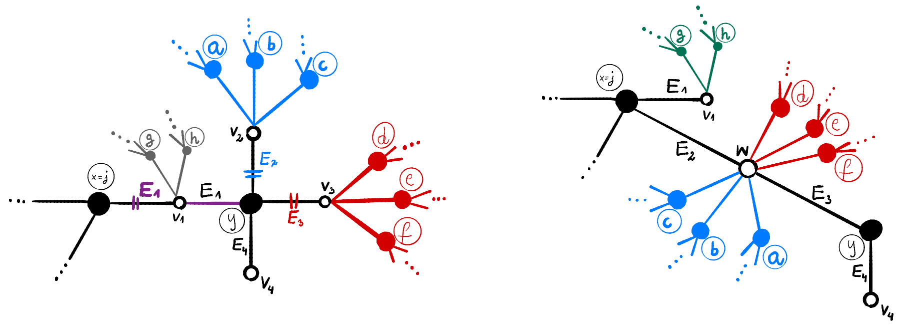

(a) (b)

Figure 9. (a) The initial configuration of the tree in the special case when $j = x$. (b) The output of $\mathbb{J}_{x,y}$ in the special case when $j = x$.

We also connect the new vertex w to the vertex y by a new edge which we label E_3; the position of the edge E_3 in the vertex y replaces the three edges which were removed from y. Again, this newly created edge replaces the removed edge between y and v_3, so if this removed edge was the root of the cluster E_3, we declare that the new edge E_3 becomes now the new root of the cluster E_3.

We merge the vertices v_2 and v_3 with the vertex w. More specifically, the clockwise cyclic order of the edges around the vertex w is as follows: the edge E_2, then the edges from the vertex V_3 (listed in the clockwise order starting from the removed edge E_3; on Figures 8 and 9 these edges are marked red), the edge E_3, then the edges from the vertex v_2 (listed in the clockwise order starting from the removed edge E_2; on Figures 8 and 9 these edges are marked blue), see Figures 8b and 9b.

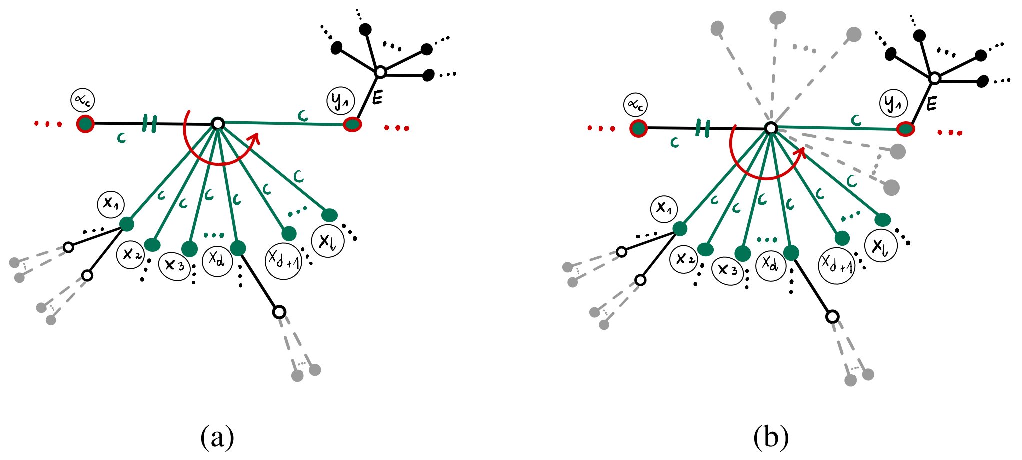

Figure 10. (a) A spine cluster c of the tree T_1 corresponding the part of the tree T_0 on Figure 3. The black vertices α_c, y_1 with $\alpha_c < y_1$ are spine vertices. The vertex α_c is the anchor of the cluster c as well as the black endpoint of the root of the cluster c. We denote by $x_d = \min B_c \backslash \{\alpha_c, y_1\}$ the vertex with the minimal label among non-spine vertices in the cluster. (b) The structure of the cluster c at a later stage of the algorithm as long as it remains untouched, see Proposition 2.5 (P2) for details.

From the following on we declare that the cluster E_1 is *touched* and also black vertex y is *touched*. It is easy to check that the output tree still fulfills the properties from Invariant 2.2.

It is easy to check that the following simple lemma holds true.

Lemma 2.4. *The jump operation separates the root and the anchor only in (at most) a single cluster. This potentially exceptional cluster is the one which with the notations of Figures 8 and 9 is denoted by E_2.*

In fact, we will use the jump operation only in the context when it indeed separates the root and the anchor in E_2; in this context E_2 will turn out to be a leftist cluster.

2.5. **The spine treatment.** For each spine cluster $C \in \mathfrak{C}$ we apply the following procedure (the final output will not depend on the order in which we choose the clusters from $\mathfrak{C}$). In the language of programmers we run the *external loop* (or the *main loop*) over the variable C. Since the spine in the tree T_1 is a path, the intersection $B_C \cap \mathcal{B}$ corresponds to the labels of the two black spine vertices of the cluster C in the tree T_1. One of these two vertices is the anchor α_C of the cluster, we denote the other one by y_1; in this way $\alpha_C < y_1$. As we will prove later (see Proposition 2.5, property (P2)), at the time of the execution of this particular loop iteration, the spine cluster C is of the form shown on Figure 10b.

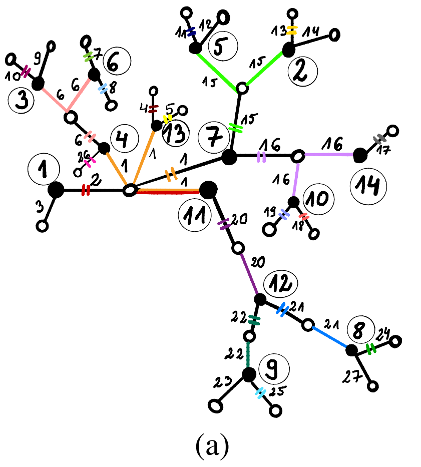
(a)

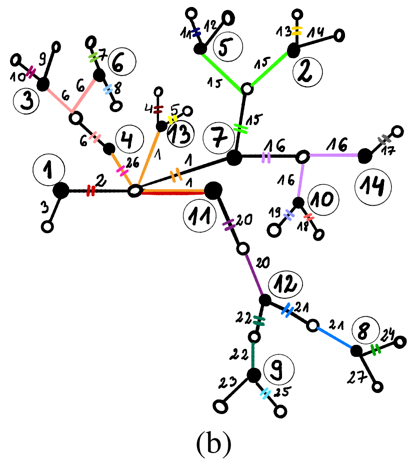
(b)

Figure 11. (a) The output of $\mathbb{B}_{1,11}$. (b) The output of $\mathbb{B}_{7,4}$.

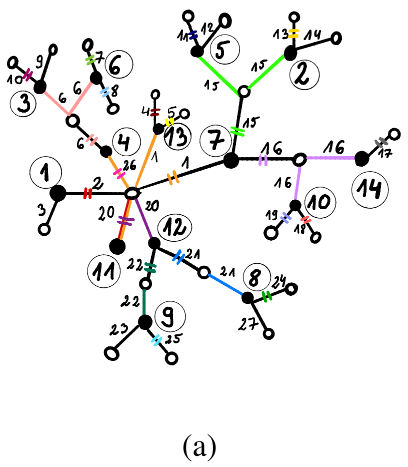
(a)

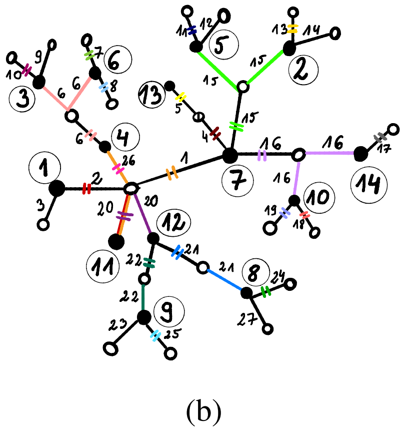
(b)

Figure 12. (a) The output of $\mathbb{B}_{7,11}$. (b) The output of $\mathbb{J}_{7,13}$.

We run the following *internal loop* over the variable $y \in B_C \backslash \{\alpha_C\}$ (with the ascending order). If $y = y_1$ or if the vertex labels $y, \alpha_C \in \{1, \ldots, n\}$ fulfill $y < \alpha_C$ then we apply $\mathbb{B}_{\alpha_C,y}$; otherwise we apply $\mathbb{J}_{\alpha_C,y}$.

Example. We continue the example from Figure 4b. We recall that $\mathfrak{C} = \{1, 2, 16\}$.

For $C = 2$ we recall that $\alpha_2 = 1$ so we have $y_1 = 11$. Since $B_2 \backslash \{1\} = \{11\}$, the internal loop is applied once with $y = 11$. As a result we apply $\mathbb{B}_{1,11}$, see Figure 11a.

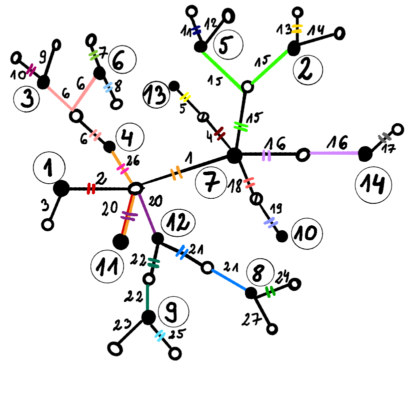

(a)

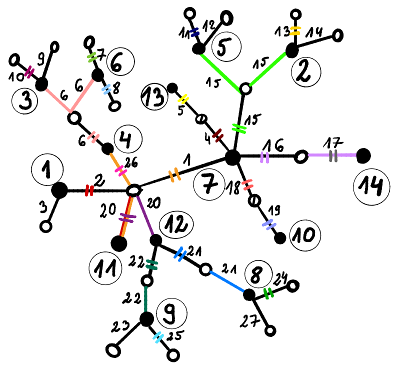

(b)

Figure 13. (a) The output of $\mathbb{J}_{7,10}$. (b) The output of $\mathbb{B}_{7,14}$.

For $C = 1$ we recall that $\alpha_1 = 7$ so we have $y_1 = 11$. Since $B_1 \backslash \{7\} = \{4, 11, 13\}$ the internal loop runs over: • $y = 4$ and we apply $\mathbb{B}_{7,4}$, see Figure 11b; • $y = 11$ and we apply $\mathbb{B}_{7,11}$, see Figure 12a; • $y = 13$ and we apply $\mathbb{J}_{7,13}$, see Figure 12b.

For $C = 16$ we recall that $\alpha_{16} = 7$ so we have $y_1 = 14$. Since $B_{16} \backslash \{7\} = \{10, 14\}$ the internal loop runs over: • $y = 10$ and we apply $\mathbb{J}_{7,10}$, see Figure 13a; • $y = 14$ and we apply $\mathbb{B}_{7,14}$, see Figure 13b.

2.6. **Correctness of the spine treatment algorithm.**

Before we present the remaining part of the algorithm (in Section 2.7) we will show that the above spine treatment is well-defined in the sense that the assumptions for the bend and jump operations (Sections 2.3.1 and 2.4.1) are indeed fulfilled during the spine treatment. We will show the following stronger result.

Proposition 2.5. *At each step of the spine treatment algorithm, the current value of the tree T fulfills the following properties.*

(P1) The tree T fulfills the properties described in Invariant 2.2.

(P2) Let c be a spine cluster of the initial tree T_1; we denote by α_c, y_1 the black spine vertices in this cluster with $\alpha_c < y_1$. Assume that the cluster c is still untouched in the tree T.

Then the vertex α_c is both the anchor of the cluster c as well as the black endpoint of the root of the cluster c.

Additionally, we compare:

(i) the cyclic order of the black vertex labels of the edges surrounding the center of the cluster c in the original tree T_1 (i.e. the cyclic order of the black endpoints' labels of the cluster c in T_1), see Figure 10a

with

(ii) the cyclic order of the black endpoints' labels of the edges surrounding the center of the cluster c in the tree T, see Figure 10b.

Then (ii) is obtained from (i) by adding some additional vertices which do not belong to the cluster c; with respect to the cyclic order these additional vertices are neighbors on either sides of the vertex y_1, see Figure 10.

(P3) The set of clusters which are touched *coincides with the set of values which the variable C (in the external loop of the spine treatment algorithm) took in the past.*

(P4) For each bend *operation (respectively, for each* jump *operation) performed during the spine treatment algorithm the assumptions (B1)–(B3) (respectively, the assumptions (J1)–(J4)) are fulfilled; in this way each* bend/jump *operation is well-defined.*

Proof. In the first part of the proof we will show that (B3), (J3) and (J4) are fulfilled in each step of the spine treatment.

Note that during the spine treatment algorithm we perform operations $\mathbb{B}_{x,\cdot}$ and $\mathbb{J}_{x,\cdot}$ for $x \in \mathcal{B}$. From the very beginning each black spine vertex is touched, so the assumption (J4) is fulfilled in each step of the spine treatment.

In order to show (B3) and (J3) we will use the observation that when one of the operations $\mathbb{B}_{\cdot,y}$ or $\mathbb{J}_{\cdot,y}$ is performed, the degree of each black vertex which is different from y increases or remains the same.

Consider some black vertex y of the initial tree T_1 which does not belong to the spine. In this case the vertex y belongs to at most one spine cluster, so during the spine treatment algorithm we perform at most one operation of the form $\mathbb{B}_{\cdot,y}$ or $\mathbb{J}_{\cdot,y}$. Therefore, the degree of y (at the time when this $\mathbb{B}_{\cdot,y}/\mathbb{J}_{\cdot,y}$ operation is performed) is at least $a_y = b_y + 2 \geqslant 3$, as required.

Consider now some black vertex y of the initial tree T_1 which belongs to the spine. In this case the vertex y belongs to at most two spine clusters. It follows that we perform no operations of the form $\mathbb{J}_{\cdot,y}$ at all, and we perform at most two operations of the form $\mathbb{B}_{\cdot,y}$. In the case when we perform one such an operation $\mathbb{B}_{\cdot,y}$, the assumption (B3) is fulfilled because the degree of y at the time when this operation is performed is at least $a_y \geqslant b_y + 1 \geqslant 2$, by the same argument as in the previous paragraph. The other case when two such bend operations $\mathbb{B}_{\cdot,y}$ are performed can occur only if $y \notin \{1, n\}$ is not one of the endpoints of the spine; it follows therefore that the initial degree of the vertex y is equal to $a_y = b_y + 2 \geqslant 3$. The bend operation $\mathbb{B}_{\cdot,y}$ decreases the degree of the black vertex y by 1. Therefore, at the time when the first operation $\mathbb{B}_{\cdot,y}$ performed, the degree of y is at least $a_y \geqslant 3$ while when the second such an operation is performed, the degree y is at least $a_y - 1 \geqslant 2$, as required. This concludes the proof that the assumptions (B3) and (J3) are fulfilled in each step of the spine treatment algorithm.

In the second part of the proof, in order to show (P1)–(P4) we will use induction over the variable C in the main loop of the spine treatment algorithm. Our inductive assumption is that at the time when the iteration of the main loop starts or ends, the properties (P1)–(P3) are fulfilled.

The induction base. The input tree T_1 clearly fulfills the conditions (P1)–(P3).

The inductive step. We consider some moment in the action of the spine treatment algorithm when a new iteration of the external loop begins. By the inductive assumption the current value of the tree T fulfills the conditions (P1)–(P3). We denote by C the current value of the variable over which the external loop runs. The assumption (P3) implies that the cluster C is untouched; it follows that the assumption (P2) is applicable to this cluster and hence the cluster C has the form shown on Figure 10b. We denote by $x_1, \dots, x_l$ the non-spine vertices of the cluster listed in the counterclockwise order, cf. Figure 10, and by $x_d = \min B_C \setminus \{\alpha_C, y_1\}$ the vertex with the minimal label among non-spine black vertices in this cluster.

We will follow the action of the internal loop (over the variable y) and we will show that in each step the properties (P1), (P2) and (P4) are fulfilled. A straightforward analysis shows that the variable y in the internal loop will take the following values (listed in the chronological order):

$$\underbrace{x_d, x_{d+1}, \dots, x_l}_{\text{phase (I)}}, \underbrace{x_1, x_2, \dots, x_i}_{\text{phase (II)}}, \underbrace{\quad y_1 \quad}_{\text{phase (III)}}, \underbrace{x_{i+1}, \dots, x_{d-1}}_{\text{phase (IV)}}$$

(note that in the exceptional case when $d = 1$ this list has a slightly different form which also depends whether $x_1 < \alpha_C$ or not), therefore the execution of the internal loop can be split into the following four phases:

(I) some number of the bend operations of the form $\mathbb{B}_{\alpha_C,\cdot}$,
(II) some number of jump operations $\mathbb{J}_{\alpha_C,\cdot}$,
(III) one bend operation $\mathbb{B}_{\alpha_C,y_1}$,
(IV) some more jump operations $\mathbb{J}_{\alpha_C,\cdot}$.

For proving (P4) note that the conditions (B3), (J3) and (J4) are already proved; thus in order to show that all bend/jump operations are well-defined, it is enough to show (B1) and (B2), respectively (J1) and (J2). In the following we will analyze the phases (I)–(IV) one by one and we will check that it is indeed the case. The evolution of the cluster C over time in these four phases is shown on Figures 10b and 14 to 16 with $c := C$.

We start with the first bend operation from the phase (I), namely $\mathbb{B}_{\alpha_c,x_d}$. (Note that in the exceptional case when $d = 1$ and $x_1 > \alpha_c$ the phase (I) is empty and there is nothing to prove.) The assumptions (B1)–(B2) are clearly fulfilled for this first operation, see Figure 10b. Looking at Figure 14a, it is easy to verify that the bend operation preserves

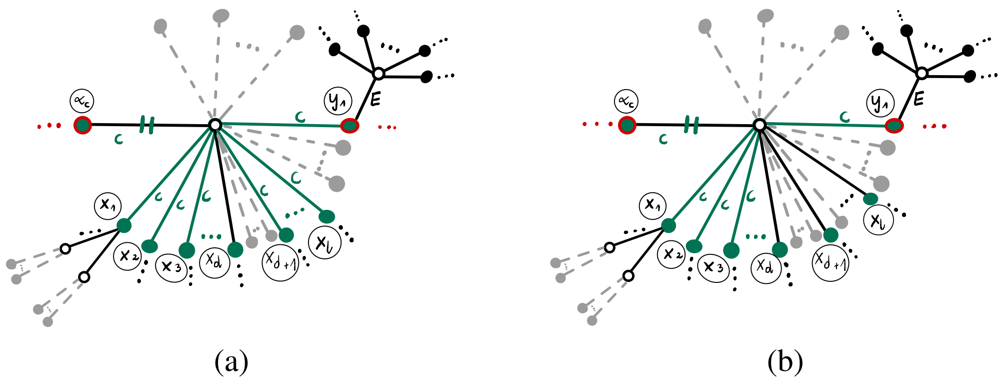

Figure 14. (a) The structure of the spine cluster c from Figure 10b after performing the first bend operation in the phase (I), namely $\mathbb{B}_{\alpha_c,x_d}$. This figure was obtained from Figure 10b by adding some additional vertices which do not belong to the cluster c; going counterclockwise these additional vertices occur after x_d and before x_{d+1}.
(b) The structure of the cluster c after the completion of the phase (I). This figure was obtained from (a) by adding some additional vertices which do not belong to the cluster c; going counterclockwise these additional vertices occur after x_{d+i} and before x_{d+i+1} for each $i \in \{1,\dots,l-d-1\}$, as well as after x_l and before y_1.

the properties from Invariant 2.2. We do not modify any other spine clusters, so also the assumption (P2) is preserved for this first bend operation.

It is easy to check that the above arguments remain valid also for the remaining bend operations from the phase (I).

We move on to the first jump operation $\mathbb{J}_{\alpha_C,x_1}$ from the phase (II). The assumptions (J1)–(J2) are clearly fulfilled for this operation $\mathbb{J}_{\alpha_C,y}$, see Figure 14b. (In the exceptional case if (a) $d=1$ and $x_1<\alpha_C$, or (b) $y_1<x_1$ the phase (II) is empty and there is nothing to prove.) Looking at Figure 15a, also it is easy to verify that this jump operation preserves the properties from Invariant 2.2. We do not modify any other spine clusters, so the assumption (P2) is still fulfilled. Also the assumptions (B1)–(B2) for the operation $\mathbb{B}_{\alpha_C,y_1}$ in the cluster C are still fulfilled.

It easy to check that the above arguments remain valid also for the remaining jump operations from the phase (II).

The phase (III) consists of the single bend operation $\mathbb{B}_{\alpha_C,y_1}$, see Figure 15b. Going counterclockwise around y_1 we denote by E the label of the edge which is immediately after the edge C, see Figure 15b. We remind that each bend operation preserves the

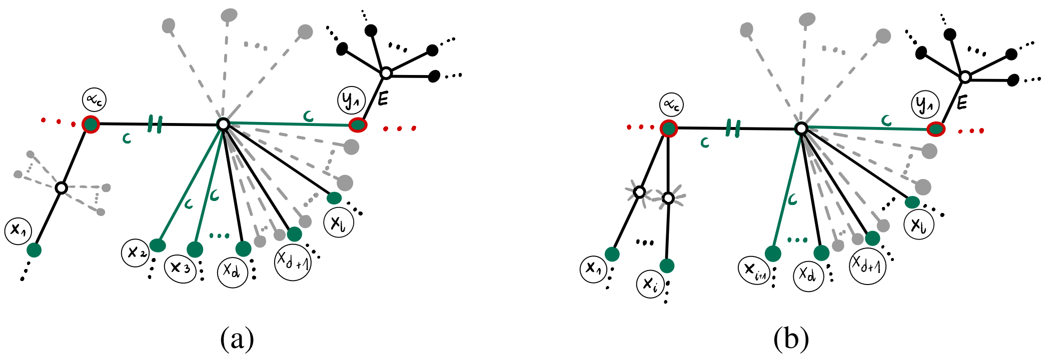

Figure 15. (a) The structure of the spine cluster c from Figure 14b after performing the first jump operation in the phase (II). This figure was obtained from Figure 14b by removal of the edge c with its black endpoint x_1 from the center of the cluster c and by combining black x_1 and α_c with a new white vertex.
(b) The structure of the cluster c from (a) after completion of the phase (II). This figure is obtained from (a) by removal of the edge c with its black endpoint x_k from the center of the cluster c and by combining black x_k and α_c with a new white vertex for each $k \in \{2, \dots, i\}$.

properties from Invariant 2.2. From Figure 16, it is easy to see that if the cluster E is non-spine or spine and touched, then we do not disturb no other untouched spine clusters, so the assumption (P2) is still fulfilled. If E is an untouched spine cluster, then either (a) the vertex y is both the anchor of the cluster E as well as the black endpoint of the root of the cluster E, or (b) y is the black spine vertex of the cluster E with the larger label. In both cases, the untouched spine cluster E still fulfills (P2).

Finally, we move on to the phase (IV); the arguments which we used in the phase (II) are also applicable here.

Note that during the execution of the internal loop we performed only operations of the form $\mathbb{B}_{\alpha_C,y}$ and $\mathbb{J}_{\alpha_C,y}$ for $y \in B_C$, so we touched exactly one cluster, namely C. Therefore, in each step of the internal loop the assumption (P3) is fulfilled. This completes the proof of the inductive step. □

2.7. **The rib treatment.**

In the current section we continue the algorithm from Section 2.5. For each successive cluster C from the sequence Σ we apply the following procedure. In the language of programming we execute an external loop over the variable C.

We run the following internal loop over the variable $y \in B_C \setminus \{\alpha_c\}$ (with the ascending order): if $y < \alpha_c$ we apply $\mathbb{B}_{\alpha_c,y}$; otherwise we apply $\mathbb{J}_{\alpha_c,y}$.

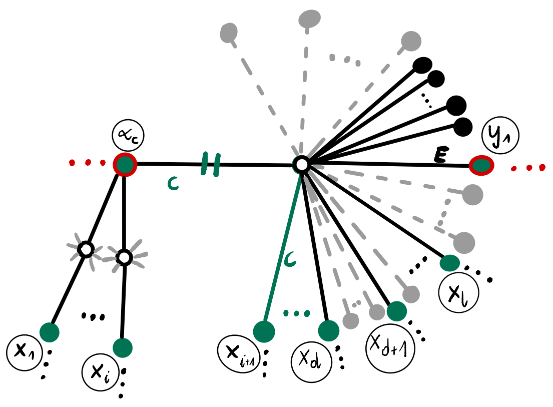

Figure 16. The structure of the cluster c from Figure 15b after performing the phase (III). The Figure 16 is obtained from Figure 15b by adding some additional vertices which do not belong to the cluster c; going counterclockwise these additional vertices occur after y_1.

Example. We continue the example from Figure 13b. We recall that $\Sigma = (6, 15, 20, 21, 22)$.

For $C = 6$ we have $\alpha_6 = 4$. Since $B_6 \backslash \{4\} = \{3, 6\}$ the loop runs over: • $y = 3$ and we apply $\mathbb{B}_{4,3}$, see Figure 17a; • $y = 6$ and we apply $\mathbb{J}_{4,6}$, see Figure 17a.

For $C = 15$ we have $\alpha_{15} = 7$. Since $B_{15} \backslash \{7\} = \{2, 5\}$ the loop runs over: • $y = 2$ and we apply $\mathbb{B}_{7,2}$, see Figure 17b; • $y = 5$ and we apply $\mathbb{B}_{7,5}$, see Figure 17b.

For $C = 20$ we have $\alpha_{20} = 11$. Since $B_{20} \backslash \{11\} = \{12\}$, the internal loop is applied once with $y = 12$. As a result we apply $\mathbb{J}_{11,12}$, see Figure 18a.

For $C = 21$ we have $\alpha_{21} = 12$. Since $B_{21} \backslash \{12\} = \{8\}$, the internal loop is applied once with $y = 8$. As a result we apply $\mathbb{B}_{12,8}$, see Figure 18b.

For $C = 22$ we have $\alpha_{22} = 12$. Since $B_{22} \backslash \{12\} = \{9\}$, the internal loop is applied once with $y = 9$. As a result we apply $\mathbb{B}_{12,9}$, see Figure 19a.

Figure 19b gives the output T_2 of our algorithm $\mathcal{A}$ applied to the minimal factorization (13). The result is a Stanley tree of type (1^{14}).

The resulting tree T_2 is the final output of our algorithm $\mathcal{A}$. In Section 3 we will show that it has the desired properties from Theorem 2.1.

2.8. **Correctness of the rib treatment algorithm.** The main result of this section is Proposition 2.7 which states that the rib treatment presented in Section 2.7 is well-defined in the sense that the assumptions for the bend and jump operations (Sections 2.3.1 and 2.4.1) are indeed fulfilled during the rib treatment.

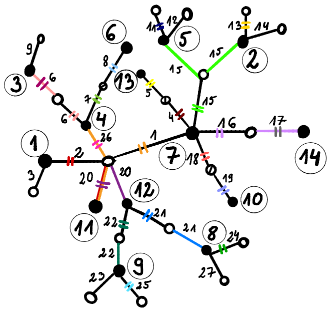
(a)

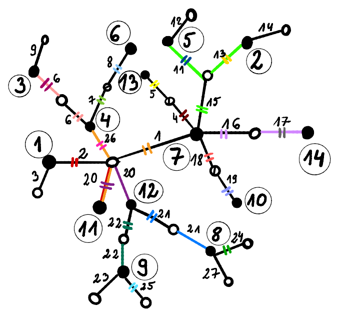
(b)

Figure 17. (a) The output of $\mathbb{B}_{4,3}$ and $\mathbb{J}_{4,6}$. (b) The output of $\mathbb{B}_{7,2}$ and $\mathbb{B}_{7,5}$.

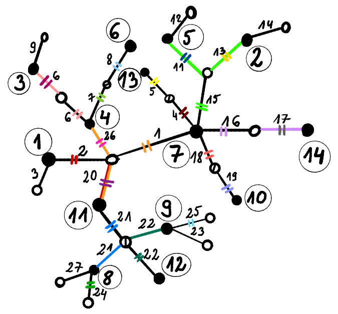
(a)

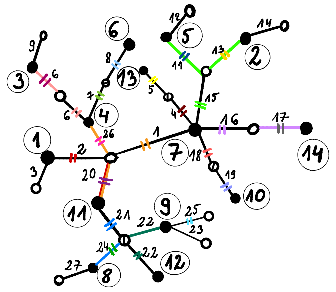
(b)

Figure 18. (a) The output of $\mathbb{J}_{11,12}$. (b) The output of $\mathbb{B}_{12,8}$.

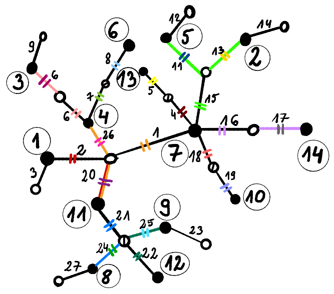
(a)

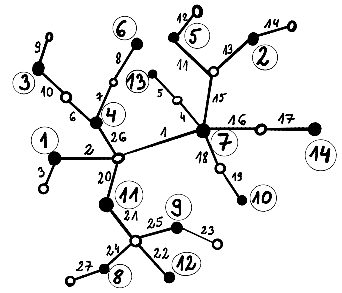
(b)

Figure 19. (a) The output of $\mathbb{B}_{12,9}$. (b) The output of our algorithm $\mathcal{A}$ applied to the minimal factorization (13).

For a black non-spine vertex z by *the branch defined by* z we mean the edge outgoing from z in the direction of the spine together with all edges and vertices which are its ancestors. The branch defined by z will also be called *the branch* z.

Lemma 2.6. *For each black non-spine vertex z the branch z does not change during the action of the algorithm $\mathcal{A}$ until the vertex z becomes touched.*

Proof. As the first step we notice that the algorithm $\mathcal{A}$ (i.e., the combined the spine part and the rib part) can be regarded as a sequence of jump and bend operations. We will use the induction over the number of bend/jump operations which have been performed so far.

At the beginning of the algorithm there is nothing to prove.

Let us take an arbitrary tree transformation $\mathbb{T}$ (with $\mathbb{T} = \mathbb{B}_{x,y}$ or $\mathbb{T} = \mathbb{J}_{x,y}$ for some black vertices x, y) in our algorithm; we denote by T the value of the tree before the transformation $\mathbb{T}$ was applied. Our inductive hypothesis is that (i) the branch z was unchanged before $\mathbb{T}$ was applied, and (ii) the vertex z was untouched before $\mathbb{T}$ was applied. Let E_1 be the cluster defined in (B1) in Section 2.3.1, respectively in (J1) in Section 2.4.1.

In the case when $z = y$ then after performing the transformation $\mathbb{T}$ the vertex z becomes touched and there is nothing to prove.

We will show that x is touched. In the case when the black vertex x in the original tree T_1 was a spine vertex there is nothing to prove. Consider now the case when x in T_1 was a non-spine vertex; in this case the operation $\mathbb{T}$ is a part of the rib treatment algorithm. Let c be the white vertex in the original tree T_1 which is the parent of the vertex x; it follows that in some moment before the operation $\mathbb{T}$ was applied, the variable in the external loop (either in the spine treatment algorithm or in the rib treatment algorithm) took the value $C = c$ and one of the operations: $\mathbb{J}_{\alpha_c,x}$ or $\mathbb{B}_{\alpha_c,x}$ was applied; since this moment the vertex x was touched, as claimed. Since z is assumed to be not touched, it follows that $z \neq x$.

The above discussion shows that we may assume that $z \notin \{x, y\}$. We denote by F the cluster in the tree T_1 which is defined by the edge outgoing from the vertex z in the direction of the spine. We will show that the cluster E_1 is not contained in the branch z, i.e., the situation depicted on Figure 20 is *not* possible. By contradiction, suppose that the cluster E_1 is contained in the branch z. By the inductive assumption, before $\mathbb{T}$ was applied, the branch z remained unchanged, so the relative position of the spine, the vertex z and the clusters E_1 and F is the same in the initial tree T_1 and in the tree T, cf. Figure 20. It follows that E_1 is a non-spine cluster; furthermore either F is a spine cluster, or F is a non-spine cluster which is a predecessor of E_1 in the sequence Σ. In particular, the transformation $\mathbb{T}$ was performed during the rib treatment part of the algorithm and the value of the variable C in the main loop at this moment was equal to $C = E_1$. In one of the previous iterations of the main loop (either in the spine treatment or in the rib treatment) the variable C took the value $C = F$; during this iteration of the loop the vertex z became touched, which contradicts the inductive hypothesis.

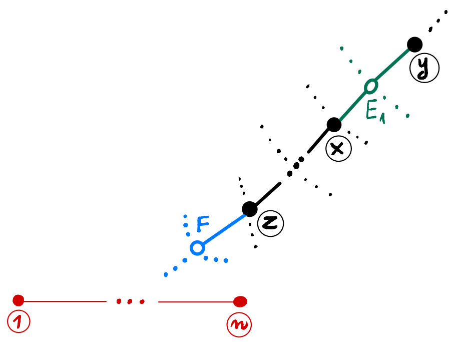

Figure 20. The hypothetical relative position of the cluster E_1 (green), the vertex z, the cluster F (blue) and the spine (red) in the tree T as long as the branch z remains unchanged.

The above observation that E_1 is *not* contained in the branch z allows us to define *the branch* z in an equivalent way by orienting all edges of the tree towards the cluster E_1 and saying that the branch z consists of the edge outgoing from z in the direction of E_1 with all edges and vertices which are its ancestors. We will use this alternative definition in the following.

In the case when $\mathbb{T} = \mathbb{B}_{x,y}$ (see Figure 7a, where z is any black vertex different than x and y; note that this black vertex may be also in the part of the tree which was not shown), we can notice that the branch z still does not change after the application of $\mathbb{T}$, see Figure 7b, as required.

In the case when $\mathbb{T} = \mathbb{J}_{x,y}$ and (with the notations from Section 2.4.1) $j = x$ (see Figure 9a, where z is any black vertex different than x and y), we can notice that the branch z still does not change after the application of $\mathbb{T}$, see Figure 9b, as required.

Consider now the remaining case when $\mathbb{T} = \mathbb{J}_{x,y}$ and $j \neq x$ (see Figure 8). If $z \neq j$ then the branch z still does not change after the application of $\mathbb{T}$, as required. The case $z = j$ is is not possible because Invariant 2.2 (I4) applied to the cluster E_1 implies that z is touched which contradicts the inductive assumption.

This completes the proof of the inductive step. □

Proposition 2.7. *For each operation* bend *(respectively,* jump*) performed during the rib treatment algorithm the assumptions (B1)–(B3) (respectively, the assumptions (J1)–(J4)) are fulfilled; in this way each* bend/jump *operation is well-defined.*

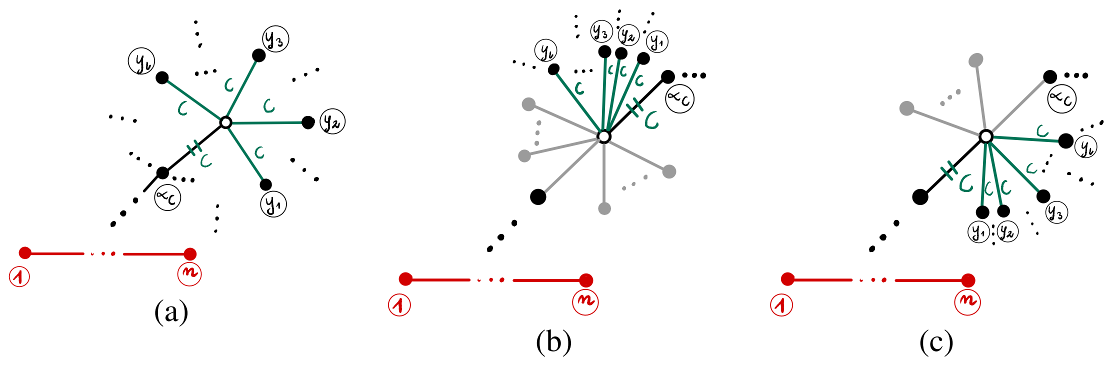

Figure 21. Three possible structures of the non-spine cluster C at the beginning of the iteration of the external loop in the rib treatment algorithm.
(a) This structure coincides with the original structure of C in the input tree T_1. The edge outgoing from the center of the cluster C in the direction of the spine is the root of the cluster C and its black endpoint is the anchor α_C of the cluster.
(b) This structure occurs as an outcome of either (i) the bend operation in the parent cluster, provided that C is the leftmost child, or (ii) the jump operation in the parent cluster, provided that C is the second leftmost child, i.e., C corresponds to E_2 with the notations from Figures 8 and 9. This structure was obtained from (a) by adding some additional vertices which do not belong to the cluster C; going clockwise these additional vertices occur after α_C. The edge outgoing from the center of the cluster C in the direction of the spine does not belong to the cluster C.
(c) This structure occurs as an outcome of the jump operation in the parent cluster, provided that C is the leftmost child, i.e., C corresponds to E_1 with the notations from Figures 8 and 9. The root edge does not correspond to any of the edges which formed C in the original tree T_1; in particular the black endpoint of the root does not belong to the set $B_C = \{\alpha_C, y_1, \dots, y_l\}$. The root of the cluster C is in the direction of the spine. More specifically, the counterclockwise cyclic order of the edges with their black endpoints around the center of cluster C is as follows: the root of the cluster C, the edges which belong to cluster C with consecutive black endpoints $y_1, \dots, y_l$, the edge which does not belong to the cluster C with the black endpoint equal to the anchor α_C and the remaining edges which do not belong to the cluster C.

Proof. We will go through some iteration of the external loop of the rib treatment for some specific value of the variable C (i.e., C is a non-spine cluster) and we will verify that all operations performed in this iteration are well-defined.

Consider the case when the anchor α_C is a non-spine vertex. By C_1 we denote the cluster which is the parent of the cluster C in the tree T_1. Therefore, the black vertex α_C also belongs to the cluster C_1. During some previous iteration of the main loop either during the spine treatment or during the rib treatment (more specifically, this was the iteration when the variable C took the value C_1) we performed an operation $\mathbb{T}$ with $\mathbb{T} = \mathbb{B}_{\alpha_{C_1},\alpha_C}$ or $\mathbb{T} = \mathbb{J}_{\alpha_{C_1},\alpha_C}$. From the above Lemma 2.6 it follows that until the operation $\mathbb{T}$ was performed, the branch defined by the black vertex α_C was unchanged, hence the cluster C had the form depicted on Figure 21a.

In the case when $\mathbb{T} = \mathbb{B}_{\alpha_{C_1},\alpha_C}$ is a bend operation, after this operation $\mathbb{T}$ is applied the cluster C either has the form depicted on Figure 21b (this happens if C is leftist) or it still has the form depicted on Figure 21a (otherwise).

In the case when $\mathbb{T} = \mathbb{J}_{\alpha_{C_1},\alpha_C}$ is a jump operation, after this operation $\mathbb{T}$ is applied the cluster C either has the form depicted on Figure 21c (this happens if C is leftist), or the form depicted on Figure 21b (this happens if C is the second leftmost child) or it still has the form depicted on Figure 21a (otherwise).

For each of the aforementioned three cases depicted on Figure 21 one can go through the internal loop (in a manner similar to that from the proof of *the inductive step* on the pages 21–23, but simpler) and to verify that the assumptions required by the bend/jump operations are indeed fulfilled, as required.

Now, we assume that α_C is a spine vertex. In this case we have two possible situations. The black vertex α_C belongs to either one or two spine clusters in the tree T_1.

Consider the case when the anchor α_C belongs to two spine clusters in the tree T_1, denoted by C_1, C_2. During some previous iteration of the main loop of the spine treatment part (more specifically, this was the iteration when the variable C took the value C_i for $i = 1, 2$) we performed an operation $\mathbb{T}$ with

(i) $\mathbb{T} = \mathbb{B}_{\alpha_{C_i},\alpha_C}$ if $\alpha_{C_i} < \alpha_C$,
(ii) $\mathbb{T} = \mathbb{B}_{\alpha_{C_i},\cdot}$ or $\mathbb{T} = \mathbb{J}_{\alpha_{C_i},\cdot}$ if $\alpha_{C_i} = \alpha_C$.

In the case (i), after this operation $\mathbb{T} = \mathbb{B}_{\alpha_{C_i},\alpha_C}$ is applied, the cluster C either has the form depicted on Figure 21b (this happens if C is leftist) or it still has the form depicted on Figure 21a (otherwise). By checking these two cases separately (the reasoning is fully analogous to the one presented above) we see that during this external loop iteration for this specific value of C all the assumptions for the bend/jump operations are fulfilled, as required.

In the case (ii), after the operation $\mathbb{T}$ is applied the cluster C still has the form depicted on Figure 21a. Again, one can easily check that that during this loop iteration all the assumptions for the bend/jump operations are fulfilled, as required.

In the case when the black vertex α_C belongs to only one spine cluster in the tree T_1 the reasoning is analogous to the one above and we skip the details. □

As an extra bonus, the above proof shows that any non-spine cluster C at a later stage of the algorithm (as long as it remains untouched) either has the form (a), (b), or (c) on Figure 21.

3. The output of the bijection is a Stanley tree

The following results are the first step towards the proof of Theorem 2.1.

Lemma 3.1. *Let $\mathbb{J}_{x,y}$ be one of the jump operations performed during the execution of the algorithm $\mathcal{A}$, and let j be the corresponding black vertex which was defined in the assumption (J2) from Section 2.4.1, see Figures 8 and 9. Then the label of the vertex j is smaller than the label of the vertex y.*

Proof. Our strategy is to explicitly pinpoint the vertex $j = j(x, y)$ in the original tree T_1.

We start with the case when the jump operation $\mathbb{J}_{x,y}$ was performed during the spine treatment (this case holds true if and only if the white vertex between x and y is a spine vertex). Let C be the value of the external loop variable at the time when $\mathbb{J}_{x,y}$ was performed. We have shown in the proof of Proposition 2.5 that the anchor of the cluster C is the endpoint of the root of the cluster C in each step of the internal loop. Therefore $j = x$, see the case described on Figure 9.

Consider now the case when the jump operation $\mathbb{J}_{x,y}$ was performed during the rib treatment; again let C be the value of the external loop variable at the time when $\mathbb{J}_{x,y}$ was performed; in particular C is a non-spine cluster.

If the cluster C in the tree T_1 is non-leftist, from Lemmas 2.3 and 2.4 we infer that no bend/jump operation separates the anchor of the cluster C with the root of this cluster, it follows therefore that $j = x$, see the case described on Figure 9.

Consider now the case when the cluster C in the tree T_1 is leftist. From Lemmas 2.3 and 2.4 it follows that in order to check whether the anchor of the cluster C is separated from the root, we need to consider one of the previous iterations of the main loop (in the spine treatment or the rib treatment), namely the one for the cluster C' which is the parent of C. In the case when $x < \alpha_{C'}$, this previous iteration contained the bend operation $\mathbb{B}_{\alpha_{C'},x}$ which does not separate the anchor from the root, so again $j = x$.

The only challenging case is the one when C is a leftist cluster and $x > \alpha_{C'}$ so that this previous iteration contains the jump operation $\mathbb{J}_{\alpha_{C'},x}$ which separates the anchor and the

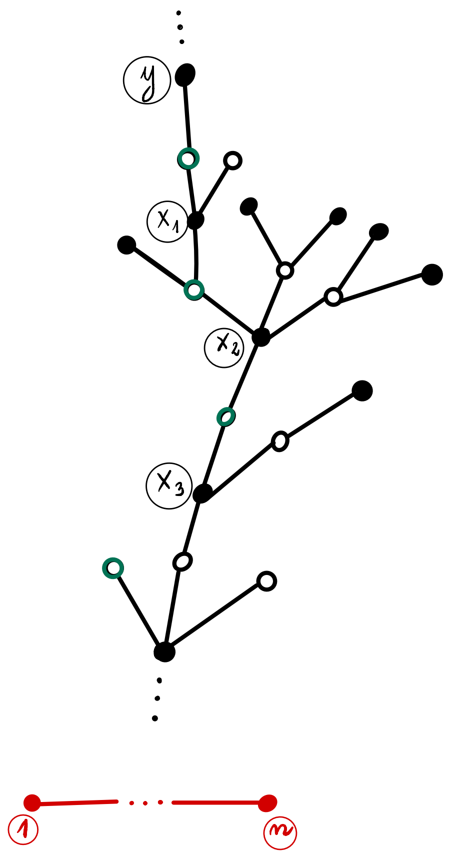

Figure 22. The tree T_1 with black vertices y, x_1, x_2, x_3 where a white leftist vertices are marked green.

root in the cluster C. Let us have a closer look on this previous jump operation $\mathbb{J}_{\alpha_{C'},x}$; it is depicted on Figures 8 and 9 with the blue cluster $E_2 = C$ and the black cluster $E_1 = C'$. Our desired value of $j(x, y)$ is the black endpoint of the root of the cluster C; on Figures 8b and 9b this endpoint carries the label j. On the other hand, the value of the variable $j = j(\alpha_{C'}, x)$ for the previous jump operation $\mathbb{J}_{\alpha_{C'},x}$ in the parent cluster is the black endpoint of the root of the cluster $C' = E_1$; on Figures 8a and 9a this vertex carries the same label j. In this way we proved that our desired value of

$$j = j(x, y) = j(\alpha_{C'}, x)$$

coincides with the value of j for the jump operation $\mathbb{J}_{\alpha_{C'},x}$ in the parent cluster. It follows that the value of j can be found by the following recursive algorithm.

We traverse the tree T_1, starting from the black vertex y, always going towards the spine, as long as the following two conditions are satisfied:

(C1) we are allowed to enter a white vertex only if it is a leftist vertex;

(C2) we are allowed to enter a black vertex only if its label is smaller than the label of the last visited black vertex so far.

Additionally, if we just entered a black spine vertex, the algorithm terminates. If we entered a white spine vertex w it is not clear what does it mean *to move towards the spine*; we declare that we should move now to the the root α_w of the cluster defined by w. We denote by $z = (z_1, \dots, z_l)$ the labels of the visited black vertices. For the example on Figure 22 if $x_3 < x_2 < x_1 < y$ we have $z = (y, x_1, x_2, x_3)$. The label z_l of the last visited black vertex is the label of our searched black vertex j. It is obvious that $j < y$. □

Proposition 3.2. *The output of the algorithm $\mathcal{A}$ from Section 2 belongs to $\mathcal{T}_{b_1,\dots,b_n}$.*

Proof. By construction, the initial tree T_1 has n black vertices labeled with the numbers $1, \dots, n$, and k white vertices, and $\sum_i a_i = n + k - 1$ edges labeled with the numbers $1, \dots, k$ in such a way that each edge label is used at least once, cf. (9). By counting the number of edges we observe that

$$\sum_{c=1}^{k} |B_c| = n + k - 1.$$

Furthermore, if $c \in \{1, \dots, k\} \backslash (\mathfrak{C} \cup \Sigma)$, so that the corresponding cluster is a leaf, then $|B_c| = 1$. It follows that the total number of *jump*/*bend* operations during the execution of our algorithm $\mathcal{A}$ is equal to

$$\begin{aligned} \sum_{c\in\mathfrak{C}} (|B_c| - 1) + \sum_{c\in\Sigma} (|B_c| - 1) &= \\ = \sum_{c\in\mathfrak{C}} (|B_c| - 1) + \sum_{c\in\Sigma} (|B_c| - 1) &+ \sum_{c\in\{1,\dots,k\}\backslash\{\mathfrak{C}\cup\Sigma\}} (|B_c| - 1) = \\ &= \left(\sum_{c=1}^{k} |B_c| \right) - k = n - 1. \end{aligned} \tag{15}$$

After performing each bend/jump operation, the number of white vertices as well as the number of edges decreases by 1; furthermore the edge which disappears has a repeated label, in this way the set of the edge labels remains unchanged in each step.

It follows that the output T_2 is a bicolored plane tree with $(n+k-1)-(n-1) = k$ edges labeled by numbers $1, \dots, k$ (so each label is used exactly once) and with $k - (n-1) = \sum_{i=1}^{n} b_i$ white vertices, cf. (4). To complete the proof we have to show that the tree T_2 is a Stanley tree of type $(b_1, \dots, b_n)$.

We will consider two types of edges: *solid* and *dashed*. At the beginning in the plane tree T_1 each edge is declared to be *solid*. After performing the operation $\mathbb{B}_{x,y}$ the two edges which form the path between x and y become *dashed*, see Figure 7b. After performing the operation $\mathbb{J}_{x,y}$ the two edges which form the path between j and y become *dashed*, see Figure 8b (for the case when $j = x$, see Figure 9b).

We say that a white white vertex v *is attracted* to a black vertex i if one of the following two conditions holds true:

- the vertices i and v are connected by a *solid* edge,
- the vertices i and v are connected by a *dashed* edge and

$$\max \big\{ y : y \textit{ and } v \textit{ are connected by a dashed edge} \big\} = i.$$

If v is attracted to i, we will also say that *the edge e between v and i is attracted to i* or that *e is an attraction edge*.

For each $i \in \{1, \dots, n\}$ we define the variable $\mathfrak{b}_i$; in each step of the algorithm this variable counts the number of white white vertices which are attracted to the black vertex i.

By considering any bend/jump operation which is performed during the algorithm $\mathcal{A}$ it is easy to see that each of the variables $\mathfrak{b}_1, \dots, \mathfrak{b}_n$ weakly decreases over time. The only difficulty in the proof is to verify that during the jump operation the newly created vertex w (with the notations from Figures 8 and 9) is not attracted to the vertex j; this fact is a consequence of Lemma 3.1. Below we will show that for $i \in \{2, \dots, n-1\}$ the variable $\mathfrak{b}_i$ during the algorithm $\mathcal{A}$ decreases at least by 2, while each of the variables $\mathfrak{b}_1$ and $\mathfrak{b}_n$ decreases at least by 1.

Case 1: i is a non-spine vertex. For convenience we will denote the non-spine black vertex i by the symbol y. There exists exactly one cluster $c \in \{1, \dots, k\}$ in the direction of the spine in the plane tree T_1 such that $y \in B_c$. In the iteration of the main loop (in the spine treatment or in the rib treatment) corresponding to $C = c$ one of the following operations is applied: either $\mathbb{B}_{\alpha_c,y}$ (if $y < \alpha_c$, see Figure 23) or $\mathbb{J}_{\alpha_c,y}$ (otherwise, see Figure 24). By Lemma 2.6 it follows that at the time one of these operations is applied, the edges in the branch y are solid; on Figures 23a and 24a this branch is located on the right-hand side and drawn with non-wavy lines. By looking on Figures 23 and 24 we see that for either of these two operations $\mathfrak{b}_y^{\text{after}} = \mathfrak{b}_y^{\text{before}} - 2$, as required.

Case 2: i is a spine vertex. Note that in the spine treatment any two bend operations commute. Furthermore, any jump operation performed in a given spine cluster does not affect the remaining spine clusters. Therefore, the final output does not depend on the order in which we choose the clusters from $\mathfrak{C}$. For this reason we may start the analysis of the time evolution of any spine cluster C from the input tree T_1 where all edges are solid (i.e., we may assume that the external loop is executed first for the cluster C).

If $i \in \mathcal{B} \backslash \{1, n\}$ is not one of the endpoints of the spine, it belongs to exactly two spine clusters c_1, c_2 in the plane tree T_1. Let us fix some $j \in \{1, 2\}$; with the notations of

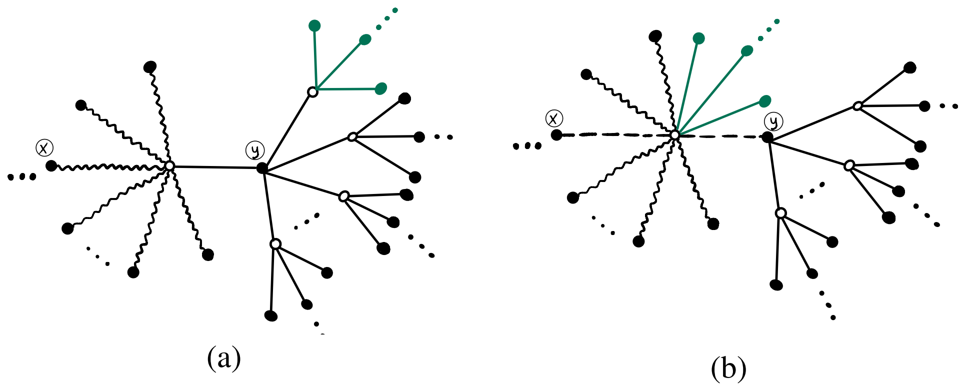

Figure 23. (a) The initial configuration of the tree. Wavy edge means that this edge can be *solid* or *dashed*.
(b) The structure of the tree (a) after performing the operation $\mathbb{B}_{x,y}$ with $x > y$.

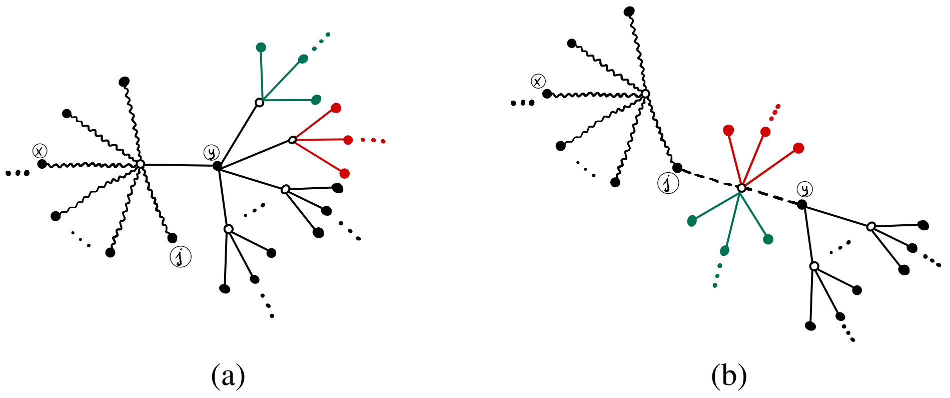

Figure 24. (a) The initial configuration of the tree. Wavy edge means that this edge can be *solid* or *dashed*. We recall that $j < y$ by Lemma 3.1.
(b) The structure of the tree (a) after performing the operation $\mathbb{J}_{x,y}$ with $x < y$.

Figure 10a, $i \in \{\alpha_{c_j}, y_1\}$ is one of the two spine vertices in the cluster c_j and $\mathbb{B}_{\alpha_{c_j},y_1}$ is one of the operations which is performed in the iteration of the external loop in the spine treatment for $C = c_j$. From Figure 25 it follows that for each spine vertex $v \in \{\alpha_{c_j}, y_1\}$ in this cluster $\mathfrak{b}_v^{\text{after}} = \mathfrak{b}_v^{\text{before}} - 1$. Since there are two choices for $j \in \{1,2\}$ it follows that the variable $\mathfrak{b}_i$ decreases (at least) twice during the whole algorithm, as required.

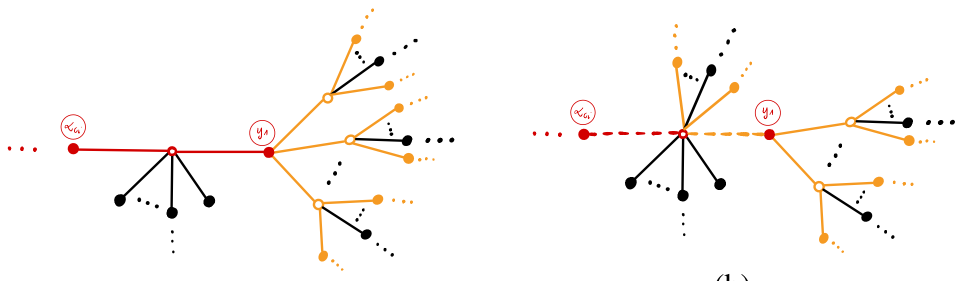

(a) (b)

Figure 25. (a) The initial configuration of the tree T_1. The black vertices α_{c_i}, y_1 are spine and such that $\alpha_{c_i} < y_1$. The orange edges mark one of the possible pathways of the spine.
(b) The structure of the tree (a) after performing the operation $\mathbb{B}_{\alpha_{c_i}, y_1}$.

An analogous argument shows that if $i \in \{1, n\}$ is one of the endpoints of the spine then the variable $\mathfrak{b}_i$ decreases (at least) once during the whole algorithm, as required.

At the beginning of the algorithm $\mathfrak{b}_i^{\text{initial}} = a_i$ for each $i \in \{1, \dots, n\}$; the above discussion shows therefore that in the output tree T_2

$$\mathfrak{b}_1^{\text{final}} \leqslant a_1 - 1, \quad \mathfrak{b}_2^{\text{final}} \leqslant a_2 - 2, \quad \dots, \quad \mathfrak{b}_{n-1}^{\text{final}} \leqslant a_{n-1} - 2, \quad \mathfrak{b}_n^{\text{final}} \leqslant a_n - 1. \tag{16}$$

It follows that

$$\sum_{i=1}^{n} \mathfrak{b}_i^{\text{final}} \leqslant \sum_{i=1}^{n} (a_i - 1) - (n-2) = (k-1) - (n-2) = k - (n-1),$$

where we used the relationship (9). In each step of the algorithm each white vertex is attracted to at least one black neighbor; it follows that the left-hand side of the above inequality is an upper bound for the number of white vertices in the output tree T_2.

On the other hand, from the first part of the proof we know that the output tree T_2 has exactly $k - (n-1)$ white vertices and the above inequality is saturated:

$$\sum_{i=1}^{n} \mathfrak{b}_i^{\text{final}} = k - (n-1). \tag{17}$$

It follows that each white vertex is attracted to exactly one black neighbor; also the tree T_2 is a Stanley tree of type $(\mathfrak{b}_1^{\text{final}}, \dots, \mathfrak{b}_n^{\text{final}})$. If at least one of the inequalities (16) was strict, this would contradict (17). We proved in this way that $\mathfrak{b}_i^{\text{final}} = b_i$ which is given by (12) which completes the proof. □

4. Alternative description of the bijection

In the current section we will provide an alternative description of the bijection $\mathcal{A}$. This alternative viewpoint on $\mathcal{A}$ will be essential for the construction of the inverse map $\mathcal{A}^{-1}$ in Section 5.

Recall that the *spine* in the output tree T_2 is the path connecting the two black vertices with the labels 1 and n. We orient the non-spine edges of the tree T_2 in the direction of the spine. In this way we can view the plane tree T_2 as a path (=the spine) to which there are attached plane trees. With this perspective in mind, the output tree T_2 will turn out to be uniquely determined by: the *'local information'* about the structure of white non-spine vertices, the *'local information'* about the structure of black non-spine vertices, and the information about the spine and its small neighborhood. The aforementioned *'local information'* for a black non-spine vertex y is just the list of the labels of the edges connecting y to its children. For a white non-spine vertex the *'local information'* contains more data, see Section 4.2. This local information will be provided separately for white non-spine vertices (Sections 4.1 to 4.4) and for certain black non-spine vertices (Section 4.6). Finally, in Sections 4.9 and 4.10 we will describe the spine vertices of T_2 as well as its neighborhood.

4.1. **White vertices: organic versus artificial.**

Recall that in the description of the jump operation in Section 2.4.2 the newly created white vertex w (see Figures 8b and 9b) was declared to be *artificial*. Each white vertex which was *not* created in this way by some jump operation will be referred to as *organic*. More precisely, we declare that all white vertices in the initial tree T_1 are organic. The bend operation can be viewed as merging two white vertices (with the notations of Figure 7a these are the vertices v_1 and v_2); it turns out that for each bend operation which is performed during the execution of the algorithm the vertex v_2 is organic. We declare that the vertex created by merging v_1 and v_2 is organic (respectively, artificial) if and only if v_1 was organic (respectively, artificial).

4.2. **Direct neighborhood of a white non-spine vertex.**

For any non-spine white vertex w of T_2 we will describe *the direct neighborhood of* w which is defined as:

- the labels of the children of w, together with the labels of the corresponding edges, and
- the label of the *parental edge of* w, defined as the edge which connects w with its parent (however, we are not interested in the label of this parent).

We will describe such direct neighborhoods separately for white non-spine organic vertices and for white non-spine artificial vertices.

4.3. **Direct neighborhood of white non-spine organic vertices in the output tree T_2.**

Our starting point is the tree T_1. Our goal in this section is to find all non-spine organic white vertices in T_2 and then for each such a vertex to describe its direct neighborhood. For this reason we disregard now all artificial white vertices as well as the information about the descendants of the black vertices.

4.3.1. *The first pruning.* With this quite narrow perspective in mind, each jump operation (with the notations from Figures 8 and 9) can be seen as removal of the edge E_1 between y and v_1 as well as removal of the white vertices v_2 and v_3. The remaining children of y (i.e., the white vertices $v_4, v_5, \dots$) remain intact, but we are not interested in keeping track of the parents of white vertices (we are interested in keeping track of just the label of the parental edge for a white vertex). Still keeping our narrow perspective in mind, it follows that the application of all jump operations in the rib treatment part of the algorithm (Section 2.7) is equivalent to the following *first pruning procedure*:

> *for each non-spine white vertex v_1 and its child y which carries a bigger label than its grandparent (i.e., $y > \alpha_{v_1}$) we remove:*
> - *the vertex y together with the edge which points towards its parent,*
> - *the two leftmost children of y (with the notations of Figures 8 and 9 they correspond to v_2 and v_3) together their children, and the edges which connect them.*

The side effect of the removal of the vertex y is that each of the edges $E_4, E_5, \dots$ (which formerly connected y to its non-two-leftmost children) has only one endpoint, namely the white one.

Remark 4.1. Later on we will use the following observation: our initial choice of the cyclic order of the edges around white vertices (Section 2.1.1) implies that after this pruning, for each white non-spine vertex w the labels of its remaining children are arranged in an increasing way from right to left; furthermore, each of these labels is smaller than the label of the parent of w, i.e., α_w.

4.3.2. *The second pruning.* If an edge between a non-spine white vertex w and its child b still remains after the above pruning procedure, this means that during the execution of the algorithm $\mathcal{A}$ a bend operation $\mathbb{B}_{\alpha_w, b}$ was performed. With the notations of Figure 7a this operation does not affect the white vertices $v_3, v_4, \dots$ (i.e., the children of the vertex $y = b$ except for the leftmost child). With our narrow perspective in mind, we are not interested in keeping track of the parent of these vertices which motivates the following *second pruning procedure*:

> *we disconnect each black non-spine vertex b from the edges connecting b with each of its children, with the exception of the leftmost child.*

Again, as an outcome of this disconnection there are some edges which have only one endpoint, a white one.

Note that since in the initial tree T_0 the degree of each black vertex was at least 2, in the outcome of the second pruning each black non-spine vertex has degree equal exactly 2. Our

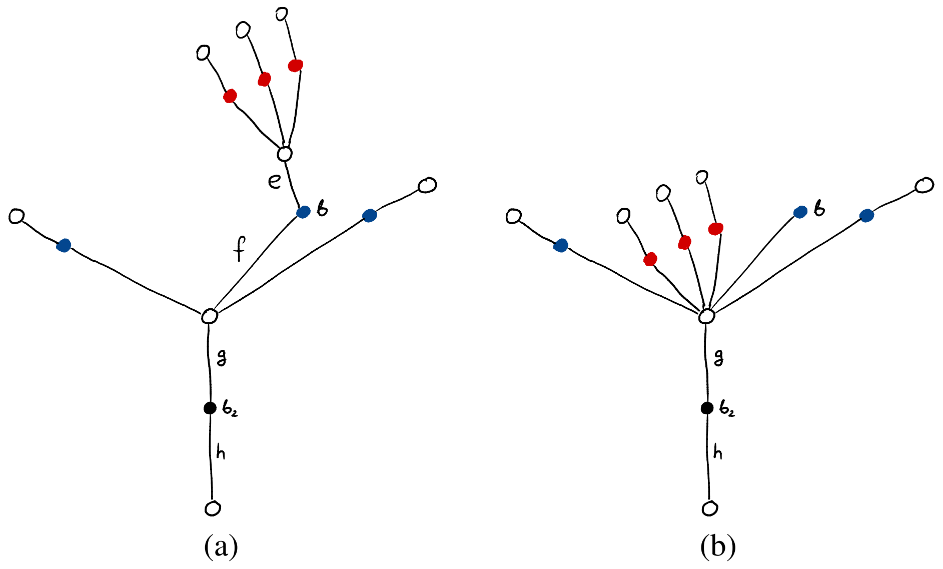

Figure 26. (a) The initial configuration of a part of the tree T. (b) The outcome of folding at the vertex b.

analysis of the impact of the bend operation $\mathbb{B}_{\alpha_w,b}$ is not complete yet and will be continued in a moment.

4.3.3. *Folding.* After performing the above two pruning operations, the tree splits into a number of connected components. Let T be one of these connected components which is disjoint with the spine; it is an oriented tree which has a white vertex v as the root. Additionally, this root v has a special edge (*the parental edge*) which is pointing in the former direction of the spine; this edge has only one endpoint.

Consider some black vertex $b \in T$. Its degree is equal to 2 and the aforementioned bend operation $\mathbb{B}_{\alpha_w,b}$ can be seen as a counterclockwise rotation of the edge which connects b with its only child towards the edge which connects b with its parent so that these two edges are merged into a single edge (see Figure 26). We keep only the label of the edge which formerly connected b with its child. As a result of the edge merging, a pair of white vertices: the child of b and the parent of b is merged into a single white vertex and the vertex b becomes a leaf. After the above *folding procedure* is applied iteratively to all black vertices in T, the connected component T becomes a single white vertex connected to a number of black vertices, and together with the parental edge of the root. For an example, see Figure 27.

The above folding procedure can be described alternatively as follows: we traverse the tree T by the depth-first search, starting at the root and touching the edges by the left

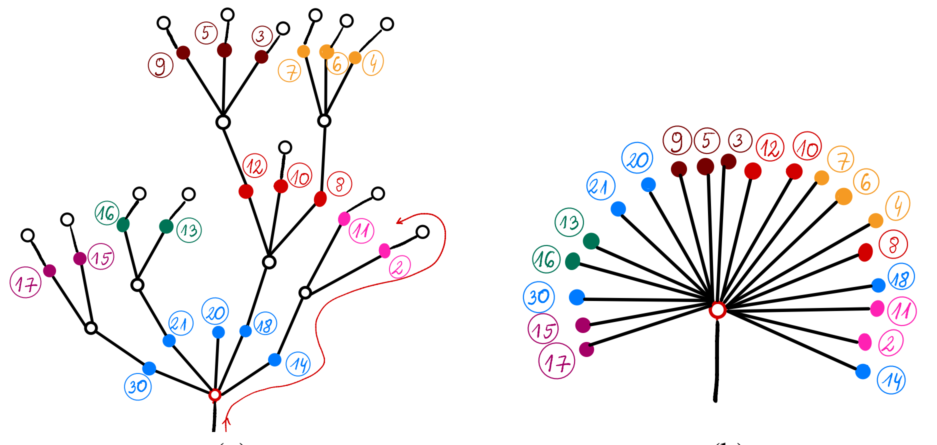

Figure 27. (a) Example of a connected component T (with a white root) of the output of the two pruning procedures. For simplicity the edge labels are not shown. The black vertices having the same parent were drawn with the same color. The thin red line with the arrows indicates the beginning of the depth-first search traversing of the tree; the black vertices are visited in the order $14, 2, 11, 18, 8, 4, \dots$ (only the first visit in a given vertex is listed). (b) The output of the folding procedure applied to the tree T from (a).

hand. For example, the beginning of such a depth-first search is indicated on Figure 27a by the red line with an arrow. We order the black vertices according to the time of the first visit in a given vertex. This order coincides with the children of the root v (listed in the counterclockwise order) in the output of folding applied to T.

4.3.4. *Conclusion.* To summarize the current subsection: there is a bijective correspondence between (i) the white non-spine organic vertices in the output tree T_2, and (ii) the connected non-spine components of the outcome of the two pruning procedures. The children of such white organic non-spine vertices in T_2 can be found by the above depth-first traversing of the connected component. This observation will critical for the construction of the inverse map $\mathcal{A}^{-1}$.

4.4. **Direct neighborhood of white non-spine artificial vertices in the output tree T_2.**

Our goal in this section is to find all non-spine artificial white vertices in T_2 and then for each such a vertex to find its direct neighborhood.

Each white artificial vertex w is created during the execution of some jump operation $\mathbb{J}_{x,y}$ so there is a bijective correspondence between the artificial white vertices and the collection of certain pairs (x, y), where x and y are black vertices such that x is a grandparent of y

and $x < y$, cf. Figures 8 and 9. Let us fix the values of w, x, and y; we shall describe now the children of w. For this reason we will disregard in the future the descendants of the black vertices as well as the white vertices which will not be merged with w by some bend operations.

After creation, the vertex w may gain some children only by the application of some bend operations; in particular we may restrict our attention only to the descendants of the vertex w and disregard the remaining part of the tree. This observation motivates the following procedure.

> *We apply the jump operation $\mathbb{J}_{x,y}$ to the initial tree T_1; the resulting tree has a unique artificial white vertex which is denoted, as above, by w. Then we keep only the vertex w, the edge adjacent to w which is in the direction of the spine, and the descendants of w. We remove the remaining part of the tree.*

A discussion analogous to the one from Section 4.3 motivates the following first pruning procedure:

> *for each remaining white vertex w' and each its child b which carries a bigger label than its grandparent (i.e., $b > \alpha_{w'}$) we remove the vertex b and all of its descendants,*

as well as the following second pruning procedure:

> *for each remaining black vertex b and each child w' of b which is not left-most, we remove the edge between b and w' as well as the vertex w', all of its descendants, and all edges between them.*

The outcome is a tree which has the white artificial vertex w as the root. Furthermore, each black vertex has degree 2. Exactly as in Section 4.3.3, we apply folding to this tree; as a result we obtain a tree which consists of a single white vertex w as the root which is connected to some number of black vertices. Additionally, the root w is connected to the parental edge which has only one endpoint. This tree is equal to the direct neighborhood of the artificial white vertex w in the output tree T_2.

To summarize: the set of *all* neighbors of an artificial vertex w together with the information about their cyclic order looks like on Figure 28.

4.5. **Children of black vertices: how to name the white vertices?** For a given black non-spine vertex we intend to find the list of its children in the output tree T_2. Each such a child is a white non-spine vertex, and in Sections 4.3 and 4.4 we already found the collection of such vertices. Now we need some naming convention which would allow to match each child to some white vertex from Sections 4.3 and 4.4. In this way a person who has the access to the tree T_1 but has no access to the tree T_1 would still be able to distinguish

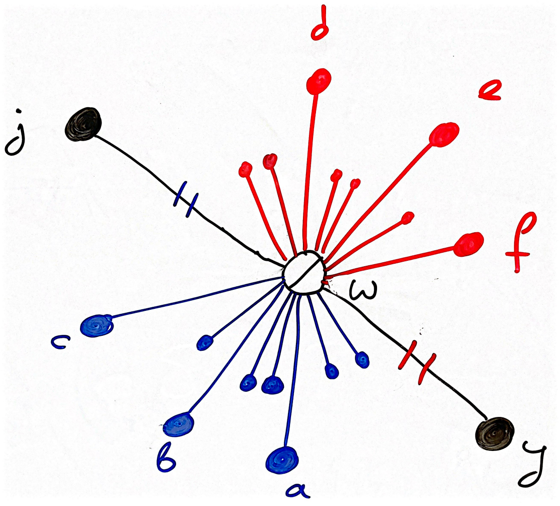

Figure 28. The neighbors of an artificial white vertex w in the output tree T_2, see Figures 8b and 9b. The vertex j is the parent of w. The blue vertices a, b, c, and the other adjacent blue vertices are the outcome of the pruning and folding of the blue tree on Figures 8a and 9a which starts with the edge E_2. The red vertices d, e, f, and the other adjacent red vertices are the outcome of the pruning and folding of the red tree on Figures 8a and 9a which starts with the edge E_3. By Remark 4.1 and Lemma 3.1 the vertex y carries the biggest label among all neighbors of w.

the white non-spine vertices of T_2. Our naming convention will be defined separately for the white organic and for the white artificial vertices.

In Section 4.3 we showed that each white organic vertex w in T_2 is an outcome of folding applied to a certain tree T; in order to name w we will identify it with the root of the tree T (which is just a white vertex in T_1).

To each white artificial vertex w of the tree T_2 we associate the largest label of its neighbors. This largest label y is an element of the set $\{1, \dots, n\}$ and can be identified with a black vertex in the tree T_1. The discussion from Section 4.4 shows that this map is injective and allows us to pinpoint uniquely each artificial white vertex; furthermore the label y has the following natural interpretation: the artificial vertex w was created by some jump operation of the form $\mathbb{J}_{\cdot,y}$.

With these conventions we will give the children of a non-spine black vertex in T_2 in the form of a list of (black and white) vertices of the tree T_1.

4.6. **Children of black never-spine vertices.** Consider a black vertex y which in the input tree T_1 was *not* a spine vertex. It turns out (we will prove it later in Sections 4.9 to 4.10) that the vertex y in the output tree T_2 is still not a spine vertex; in the following we will describe the children of y in T_2 as well as the labels on the edges connecting y with its children.

Recall that we oriented all non-spine edges in the tree T_1 towards the spine. Now, we additionally orient some spine edges in T_1 in such a way that for each white spine vertex w its parent is equal to the root α_w of the corresponding cluster. With this convention, we denote by x the grandparent of y. It follows that during the action of the algorithm $\mathcal{A}$ exactly one of the following two operations was performed: either the bend operation $\mathbb{B}_{x,y}$ (in the case when $x > y$) or the jump operation $\mathbb{J}_{x,y}$ (in the case when $x < y$).

4.7. Children of a black never-spine vertex, the case when $x > y$.

4.7.1. *The tree T.* In this case the bend operation $\mathbb{B}_{x,y}$ was performed. As a result, the edge connecting y to its leftmost child in T_1 is *not* among the edges which connect y to its children in T_2. The other (i.e., the non-leftmost) edges connecting y to its children in T_1 will remain in T_2; these edges will connect y to its organic children. On the other hand, the vertex y may gain some new, artificial children as an outcome of some jump operations. We will discuss them in the following.

Recall that with the notations of Figures 8 and 9 we denote by $j = j(x', y')$ the black vertex which, as a result of a jump operation $\mathbb{J}_{x',y'}$, gains a new child (which is a white artificial vertex). This vertex j is given in terms of the input tree T_1 by the algorithm contained in the proof of Lemma 3.1. The problem which we currently encounter is roughly the opposite: for a given black vertex y of T_1 we should find its all artificial children in the output tree T_2 or, equivalently, all jump operations $\mathbb{J}_{x',y'}$ performed during the algorithm for which $y = j(x', y')$. Our strategy is to construct a certain tree T which is a subtree of T_1. This plane tree will have the vertex y as the root, and it will have the following two properties:

- whenever x', y' are black vertices in T_1 such that $\mathbb{J}_{x',y'}$ is one of the operations performed during the algorithm $\mathcal{A}$ then
$$j(x', y') = y \qquad \Longleftrightarrow \qquad x', y' \in T,$$
- if x', y' are black vertices in T such that x' is the grandparent of y' then $\mathbb{J}_{x',y'}$ is one of the operations performed during the algorithm $\mathcal{A}$ (or, equivalently, $x' < y'$).

In this way there will be a bijection between the black non-root vertices of the tree T and the artificial children of the vertex y in T_2 which maps the black vertex y' to the artificial white vertex created during the operation of the form $\mathbb{J}_{\cdot,y'}$.

4.7.2. *The prunings.* As the first step towards the construction of the tree T we perform the following *zeroth pruning*:

in the tree T_1 we keep only the vertex y and its offspring.

Recall that the bend operation $\mathbb{B}_{x,y}$ was performed and the edge connecting y to its leftmost child in T_1 is *not* among the edges which connect y to its children in T_2. This motivates the following operation.

> *Additionally, we remove the label from the edge connecting y to its leftmost child.*

The condition (C2) from the algorithm contained in the proof of Lemma 3.1 motivates the following *first pruning procedure*:

> *for each remaining white vertex v_1 and its child y' which carries a* smaller *label than its grandparent we remove the edge connecting v_1 with y', as well as the vertex y' and its offspring, as well as the edges connecting them.*

Compare this to Section 4.3.1 where we removed each vertex which is *bigger* than its grandparent. As a result, the following analogue of Remark 4.1 holds true.

Remark 4.2. Later on we will use the following observation: our initial choice of the cyclic order of the edges around white vertices (Section 2.1.1) implies that after this pruning, for each white non-spine vertex w the labels of its remaining children are arranged in a *decreasing way in the clockwise order*; furthermore, each of these labels is *bigger* than the label of the parent of w, i.e., α_w.

The other condition (C1) from the algorithm contained in the proof of Lemma 3.1 motivates the following *second pruning procedure*:

> *for each remaining black vertex y' such that $y' \neq y$ is not the root vertex we remove all non-leftist children of y' as well as their offspring and all adjacent edges.*

We denote by T the outcome of these prunings. This tree has the property that the degree of each black vertex (with the exception of the root) is equal to 2.

4.7.3. *Jump operation as a replacement.* Let w be a child of the root vertex y. We start with the case when w is not the leftmost child of y. Let the black vertices $V_1, \dots, V_d$ be the children of w, listed in the clockwise order. After applying the jump operations which correspond to the cluster w the whole subtree of T which has w as the root is replaced by the following collection of trees attached to the root (we list these trees in the clockwise order):

(18) (the single organic vertex w),
(an artificial white vertex which carries the name V_1
to which there is an attached tree T_{V_1} which was formerly attached to V_1),
$\dots,$
(an artificial white vertex which carries the name V_d
to which there is an attached tree T_{V_d} which was formerly attached to V_d);

above we used the naming convention for white vertices from Section 4.5.

In the case when w is the left-most child, the above discussion remains valid, however one should remove the first entry of the list (18), i.e. the single organic vertex w.

Each tree T_{V_i} has a white vertex as the root, let the black vertices $W_1, \dots, W_e$ be is children. Now, performing all jump operations in the cluster defined by this root corresponds to replacing the following item from the aforementioned list:

(the artificial white vertex which carries the name V_i
to which there is attached tree the T_{V_i})

by the following collection of trees attached to the root y:

(the artificial white vertex which carries the name V_i),
(an artificial white vertex which carries the name W_1
to which there is an attached tree which was formerly attached to W_1),
$\dots,$
(an artificial white vertex which carries the name W_e
to which there is an attached tree which was formerly attached to W_e).

We iteratively apply these replacements until each child of the root y is a leaf. When the algorithm terminates, the ordered list of the children of the root y in the output coincides with the ordered list of the children of the vertex y in the tree T_2 that we are looking for. With the convention from Section 4.5, the children of y (listed in the clockwise order) can be identified with a list of (black and white) vertices of the input tree T_1. In the following we will provide a more direct way of finding this list based only on the tree T. In fact, the elements of the list which we construct will provide more information; each entry of the list will be a pair of the form

$$\big(\text{(name of a white vertex } w), \quad \text{(the label of the edge connecting } v \text{ and } w)\big). \tag{19}$$

4.7.4. *The depth-first search.* The recursive algorithm from Section 4.7.3 is just a complicated way of performing the depth-first search on the tree T. We traverse the tree T by keeping it with the *right*-hand side (note that in the analogous depth-first search in Section 4.3.3 we touched the tree with the *left*-hand side). When we enter a non-root vertex v for the first time, we proceed as follows:

- if v is a white vertex which is a child of the root y but not the left-most child of the root (each such a vertex corresponds to an white organic child of y in T_2), we append the list with the pair
$$\big(v, \quad (\text{the label of the edge connecting } v \text{ and } y)\big),$$
[note that during the zeroth pruning we removed the label from the leftmost edge of the root so that it is not listed here];
- if v is a black vertex (each such a vertex corresponds to a white artificial child of y in T_2) we append the list with the pair
$$\big(v, \quad (\text{the label of the edge connecting } v \text{ with its unique child in } T)\big).$$

This procedure can be regarded as an analogue of folding from Section 4.3.3. This completes the description of the *local information* about the children of a black never-spine vertex y in the case when $x > y$.

4.8. **Children of a black never-spine vertex, the case when $x < y$.** We plan to proceed in an analogous way as in Section 4.7. In this case the jump operation $\mathbb{J}_{x,y}$ was performed. As a result, the leftmost child v_2 of y (with the conventions of Figures 8 and 9) and the whole subtree attached to v_2 will not contribute to white artificial children of the vertex y. Indeed, if x', y' are black vertices, and are among the offspring of v_2 then the algorithm from the end of the proof of Lemma 3.1 for calculating $j(x', y')$ does not terminate in the vertex y and hence $j(x', y') \neq y$. For this reason our first step towards the construction of the tree T is more radical:

> *in the tree T_1 we keep only the vertex y and its offspring; additionally we remove the left-most child of y, its offspring and the adjacent edges.*

Another consequence of the aforementioned jump operation $\mathbb{J}_{x,y}$ is that the second-leftmost child of the vertex y in the tree T_1 (with the notations of Figures 8 and 9 it is the vertex v_2) will not give rise to an organic child of y in the output tree T_2. On the other hand, the subtree rooted in this second-leftmost child v_2 may give rise to some children of y which are artificial white vertices. For this reason we may proceed now with the first and the second pruning in the same way as in Section 4.7.2. Finally, the local information about the children of the black vertex y in the tree T_2 is provided by the depth-first search algorithm from Section 4.7.4.

4.9. **Detailed anatomy of the spine.**

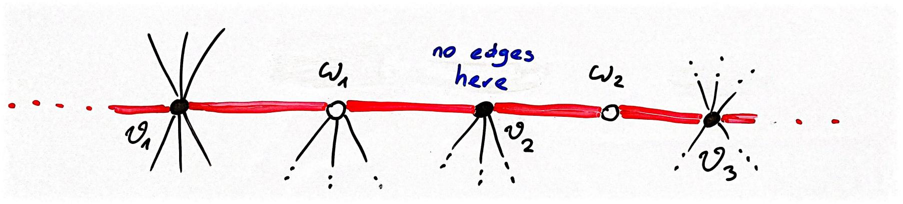

(a)

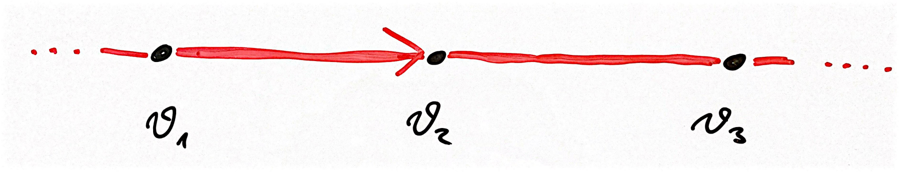

(b)

Figure 29. (a) A part of the initial tree T_1. The horizontal thick red edges are the spine, we assume that the labels of the black vertices fulfill $v_1 < v_2$. The neighbors of the white vertex w_2 are not shown. (b) The corresponding part of the backbone. The oriented edge (v_1, v_2) is bald.

4.9.1. *The backbone.* Recall that the spine in the input tree T_1 is the path connecting the two black vertices with the labels 1 and n. We define the *backbone* $\mathcal{B}$ as the graph which consists of the black spine vertices in T_1. We declare that a pair of backbone vertices $v_1, v_2 \in \mathcal{B}$ (with $v_1 \neq v_2$) is connected by an oriented edge (v_1, v_2) pointing from v_1 towards v_2 if and only if (a) the distance between v_1 and v_2 in the tree T_1 is equal to 2 (in other words, v_1 and v_2 have a common white neighbor), and (b) the labels of the vertices $v_1, v_2 \in \{1, \dots, n\}$ fulfill $v_1 < v_2$. As a result, the backbone is a path graph with 1 and n as the endpoints, together with the information about the orientation of the edges.

4.9.2. *Bald and hairy edges in the backbone.* Consider some oriented edge (v_1, v_2) in the backbone, and assume that $v_2 \neq n$ does not carry the maximal label. In this case the vertex v_2 is adjacent to another backbone vertex v_3 (with $v_3 \neq v_1$). In the tree T_1 the path between the vertices v_1 and v_3 is of the form

$$(v_1, w_1, v_2, w_2, v_3)$$

for some white vertices w_1, w_2. Assume that in the tree T_1, going clockwise around the black vertex v_2, the direct successor of the edge connecting v_2 to w_2 is the edge connecting v_2 to w_1, see Figure 29a. In this case we will say that the edge (v_1, v_2) in the backbone is *bald*, see Figure 29b. The edges in the backbone which are not bald will be called *hairy*.

4.9.3. *Maximal backbone segments.* Let $A_r, A_{r-1}, \dots, A_1, B_1, \dots, B_s \in \mathcal{B}$ (with $r, s \geqslant 1$) be backbone vertices such that:

- $(A_r, A_{r-1}),\ (A_{r-1}, A_{r-2}),\ \dots, (A_2, A_1)$ are bald edges in the backbone,
- (A_1, B_1) is a hairy edge in the backbone,
- $(B_s, B_{s-1}),\ (B_{s-1}, B_{s-2}),\ \dots, (B_2, B_1)$ are bald edges in the backbone,

see Figure 30a. We will say that the above collection of edges which form a path connecting A_r and B_s constitutes a *backbone segment*. In other words, a backbone segment consists of a single hairy edge (A_1, B_1) surrounded by two (possibly empty) oriented paths with the endpoints A_1 and B_1, which consist of only bald edges.

We say that a backbone segment is *maximal* if cannot be extended by adding an additional bald edge at either of its endpoints. It is easy to check that any two maximal backbone segments are disjoint.

We claim that each oriented edge $e = (v_1, v_2)$ of the backbone belongs to some maximal backbone segment. Indeed, if e is hairy, it forms a very short backbone segment with $r = s = 1$; by extending this backbone segment we end up with the maximal backbone segment. On the other hand, if e is bald we can follow the orientations of the edges and traverse the backbone as long as we visit only bald edges $(v_2, v_3),\ (v_3, v_4), \dots, (v_{l-1}, v_l)$. In a finite number of steps our walk will terminate; there is a number of cases which give a specific reason why the walk terminated.

Firstly, we could have encountered one of the endpoints of the backbone, i.e. $v_l \in \{1, n\}$. The case $v_l = 1$ is not possible because $v_l = 1$ carries the minimal label, so $v_l < v_{l-1}$ which contradicts the assumption that (v_{l-1}, v_l) is one of the oriented edges of the backbone. The other case $v_l = n$ is also not possible because, by definition, the oriented edge (v_{l-1}, n) is not bald.

The second possibility is that the other edge attached to the vertex v_l (it is an oriented edge of the form $f = (v_l, v_{l+1})$ or $f = (v_{l+1}, v_l)$ for some $v_{l+1} \neq v_{l-1}$)) is hairy. In this case the maximal backbone segment containing the hairy edge f contains the edge e, as required.

The third case is that the other edge attached to the vertex v_l is a bald edge $f = (v_{l+1}, v_l)$ with $v_{l+1} \neq v_l$ with the *wrong* orientation of the edge which prevents traversing f. This would imply that the backbone vertex v_l has two incoming bald edges, and therefore that the black vertex v_l (regarded as a vertex in the original tree T_1) has degree 2. On the other hand, the degree of the vertex v_l is equal to $a_{v_l} \geqslant 3$ by (12) which leads to a contradiction and completes the proof.

It follows that the maximal backbone segments provide a partition of the set of backbone edges.

4.9.4. *Tree segments.* The collection of all endpoints of the maximal backbone segments (for the maximal backbone segment depicted on Figure 30a these endpoints are denoted by

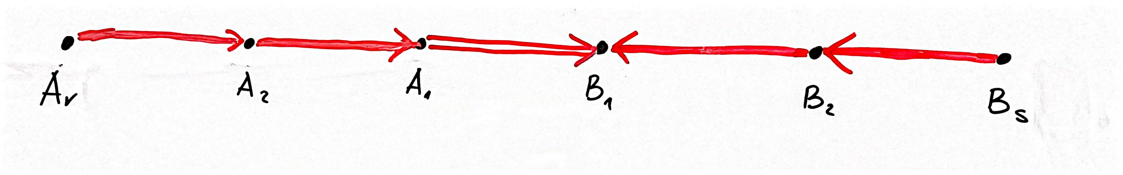

(a)

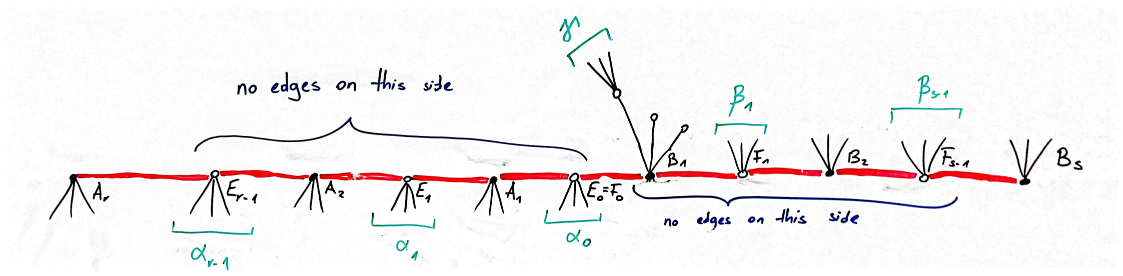

(b)

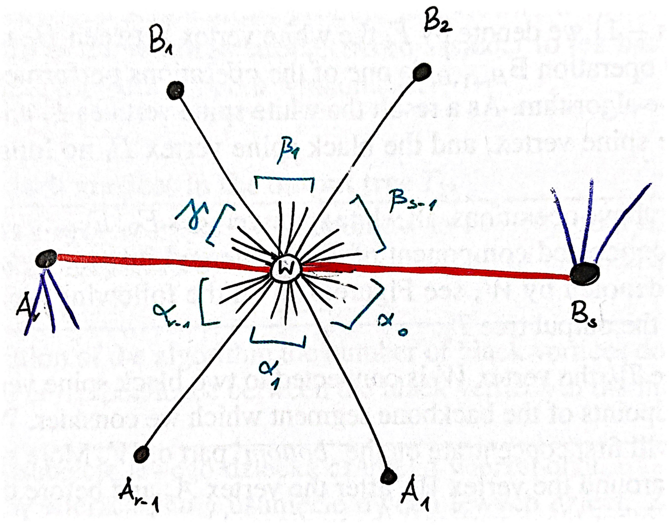

(c)

Figure 30. (a) A maximal backbone segment in the backbone. The oriented edge (A_1, B_1) is the only hairy edge on this picture, for this reason it was decorated by a double line. (b) The corresponding tree segment; for simplicity only the direct neighborhood of the spine was shown. Note that in the exceptional case $r = 1$ there is no restriction on the edges surrounding the vertex $A_1 = A_r$, and in the exceptional case $s = 1$ there is no restriction on the edges surrounding the vertex $B_1 = B_s$. (c) The outcome of the algorithm $\mathcal{A}$ applied to this tree segment. Only the neighbors of the spine white vertex W are shown.

A_r and B_s) can be used to split the initial tree T_1 into a number of connected components which will be called *tree segments*. Each such an endpoint (with the exception of the vertices 1 and n) belongs to two such tree segments; in order to split the neighbors of such boundary vertices between the two tree segments we use the convention shown on Figure 30b: each tree segment contains these non-spine edges attached at the endpoint which are on *"the left-hand side"* of the spine (from the viewpoint of a person who looks along the spine, in the direction of the respective endpoint).

The spine naturally splits the tree segments into two parts; we refer to them as *the upper part* and *the lower part* according to the convention from Figure 30b.

4.10. **Action of the algorithm on a tree segment.** In the following we will investigate the action of the algorithm on some tree segment; we will use the notations from Figure 30b.

We denote by $E_0 = F_0$ the white vertex between A_1 and B_1, and for $i \in \{1, \dots, r-1\}$ we denote by E_i the white vertex between A_i and A_{i+1}. The assumption about the orientations of the edges in the backbone segment implies that the vertex A_{i+1} is the anchor of the cluster E_i; this implies that the bend operation $\mathbb{B}_{A_{i+1},A_i}$ is one of the operations performed in the iteration of the main loop for the cluster $C = E_i$. As a result, the white spine vertices E_i and E_{i-1} are merged into a single white spine vertex. On the other hand, after this bend operation is performed, the black spine vertex A_i no longer belongs to the spine.

For $i \in \{1, \dots, s-1\}$ we denote by F_i the white vertex between B_i and B_{i+1}. Similarly as above, the bend operation $\mathbb{B}_{B_{i+1},B_i}$ is one of the operations performed during the spine treatment part of the algorithm. As a result the white spine vertices F_i and F_{i-1} are merged into a single white spine vertex, and the black spine vertex B_i no longer belongs to the spine.

As a result of the above operations, all white spine vertices $E_0, E_1, \dots, E_{r-1}, F_1, \dots, F_{s-1}$ in the considered tree segment are merged into a single white spine vertex which will be denoted by W, see Figure 30c. In the following we will describe the neighbors of W in the output tree T_2.

In the output tree T_2, the vertex W is connected to two black spine vertices: A_r and B_s which were the endpoints of the backbone segment which we consider. With the notations of Figure 30c we will first concentrate on the *'bottom'* part of W. More specifically, going counterclockwise around the vertex W, after the vertex A_r and before the vertex B_s, we encounter (among other black vertices) the vertices $A_{r-1}, A_{r-2}, \dots, A_2, A_1$, arranged in this exact order, see Figure 30c. In order to find the remaining black vertices which are interlaced in between we may revisit Section 4.3; a large part of that section is applicable also in the current context.

More specifically, for $i \in \{0, \dots, r-1\}$ we denote by α_i the part of the original tree T_1 which is attached to the spine at the white vertex E_i, see Figure 30b. Just like in Section 4.3.1 we perform the first pruning; for the purposes of this first pruning we declare that the parent of the white vertex E_i (which is the root of the tree α_i) is equal to A_{i+1}.

Then, just like in Section 4.3.2, we perform the second pruning and then the folding (see Section 4.3.3). The outcome of this procedure is a sequence of black vertices: these are exactly the neighbors of the white vertex W which appear (in the clockwise cyclic order) after the vertex A_{i+1} and before A_i; we use the convention that $A_0 = B_s$, see Figure 30c. This completes the description of the *bottom* part of the vertex W.

The *upper* part of the vertex W is slightly more complicated. We denote by γ the part of the tree T_1 which has the leftmost non-spine child of B_1 as the root, see Figure 30b. The key difference between the bottom and the upper part lies in the fact that one of the operations performed in the iteration of the main loop in the spine treatment part of the algorithm for the cluster $C = E_0$ is the bend operation $\mathbb{B}_{A_1,B_1}$. This operation plants the tree γ in the vertex W, in the counterclockwise order after the vertex B_1 and before the vertex A_r, see Figure 30c. Then the usual pruning and folding procedures are applied to γ. The remaining black vertices in the upper part of W correspond to the trees $\beta_1, \dots, \beta_{s-1}$, see Figure 30c.

As we can see, any operation performed for the clusters which form the given tree segment does not affect the other segments. For this reason it is possible to study the action of the algorithm $\mathcal{A}$ on each tree segment separately.

5. The inverse bijection

We will complete the proof of Theorem 2.1 by constructing explicitly the inverse map $\mathcal{A}^{-1}$. The starting point of the algorithm is a Stanley tree T_2 of type $(b_1, \dots, b_n)$, cf. Section 1.2. Our goal is to turn this tree into a minimal factorization $(\sigma_1, \dots, \sigma_n) \in \mathcal{C}_{a_1,\dots,a_n}$, where the numbers $a_1, \dots, a_n$ are specified in Theorem 2.1.

Similarly as in Section 2, the path in T_2 between the two black vertices with the labels 1 and n will be called *the spine*.

5.1. **Which white vertices are artificial?**

Recall that the notion of *artificial* vertices was introduced in the context of the jump operation at the beginning of Section 2.4.2. In the first step of our algorithm $\mathcal{A}^{-1}$, for a given a Stanley tree T_2 we will guess which white vertices are artificial, i.e., which vertices are the result of the jump operation. The remaining part of the current section is devoted to the details of this issue.

Lemma 5.1. *Let T_2 be an a Stanley tree which is an output of the algorithm $\mathcal{A}$ for some input data and let v be one of its white non-spine vertices. The vertex v is organic if and only if its neighbor with the maximal label is equal to the parent of v.*

With the terminology from page 33, since in the output tree T_2 all edges are dashed, each white vertex is attracted to exactly one neighbor, and the above result can be rephrased as follows: v is organic if and only if v is attracted to its parent.

Proof. Since artificial vertices arise only as a result of a jump operation, the vertex v of the tree T_2 is artificial if and only if there is a black vertex y in the tree T_2 which is a child of v and such that during the execution of the algorithm $\mathcal{A}$ there was a jump operation of the form $\mathbb{J}_{\cdot,y}$.

Consider the case when v is artificial; immediately after this jump operation is performed, the newly created vertex v (on Figure 24b it is the vertex between j and y) is attracted to y because $j < y$ by Lemma 3.1. Moreover, from the proof of the Proposition 3.2 it follows that after this jump operation $\mathbb{J}_{\cdot,y}$ is performed, the set of vertices which are attracted to y does not change until the very end of the algorithm $\mathcal{A}$. In this way v is attracted to one of its children, hence not to its parent, as required.

Consider the opposite case when v is organic; let y be some child of v. It follows that during the execution of the algorithm $\mathcal{A}$ there was a bend operation $\mathbb{B}_{\cdot,y}$. By examining Figure 23 it follows that immediately that after this bend operation was performed, the vertex v is not attracted to y. Again, from the proof of the Proposition 3.2 it follows that after this bend operation $\mathbb{B}_{\cdot,y}$ is performed, the set of vertices which are attracted to y does not change until the very end of the algorithm $\mathcal{A}$. In this way we proved that v is not attracted to any of its children, hence it is attracted to its parent, as required. □

5.2. **Recovering the cycles away from the spine.** Each black vertex $B \in \{1, \dots, n\}$ in the initial tree T_1 corresponds to the cycle σ_B. There is a canonical bijective correspondence between the set of black vertices in the tree T_1 and the set of black vertices in the output tree T_2, therefore B can be identified with a black vertex in the output tree T_2. In order to find the inverse map $\mathcal{A}^{-1}$ we need to recover the cycle σ_B based on the information contained in the tree T_2.

We will start with the assumption that the black vertex B of T_2 is away at least by two edges from the spine; this assumption will be used also in Sections 5.2 to 5.7 below.

Let W denote the parent of B, and let J denote the parent of W. We define Y to be the neighbor of W with the biggest label. Our prescription for finding σ_B will depend on the position of Y with respect to J and B, see Figure 31.

5.3. **Case (a):** $Y = J$**.** By Lemma 5.1, in this case W is an organic white vertex.

5.3.1. *The labels* $E_2, \dots, E_d$*.* The proof of Proposition 3.2 shows that the black vertex B lost exactly two white neighbors which were attracted to B when we performed the operation $\mathbb{B}_{\cdot,B}$ and it never gained new ones (we showed that $b_B = \mathfrak{b}_B^{\text{final}} = \mathfrak{b}_B^{\text{initial}} - 2 = a_B - 2$). Using this information and basing on Figure 7 (with the notations of this figure we have $y = B$, $v_1 = W$, $x = J$) we conclude that in the output tree T_2 the labels of the edges attracted to B (with the notations of Figure 7b these are the edges $E_3, \dots, E_d$) all belong to the cycle σ_B. The label of the edge which is in the direction of the spine (this edge is not attracted to B; with the notations of Figure 7b this is the edge E_2) also belongs

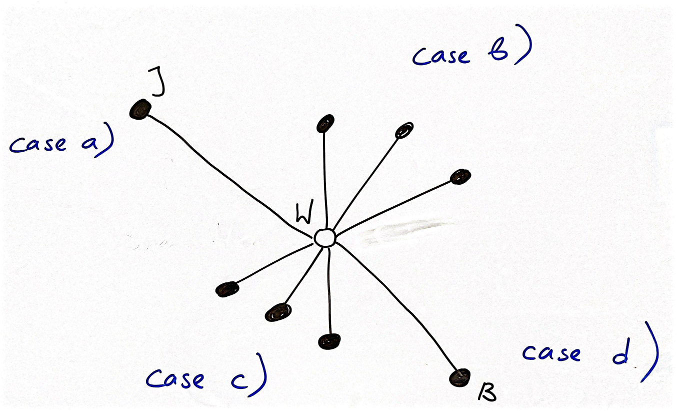

Figure 31. The four cases necessary for determining the cycle σ_B. The black vertex is assumed to be away from spine by at least two edges. The vertex W is the parent of B; the vertex J is the parent of W. We define Y to be the neighbor of W with the biggest label. The case a) (see Section 5.3) corresponds to the case when $Y = J$. The case b) (see Section 5.5) corresponds to the case when Y is located (going clockwise around the vertex W) after the vertex B and before J, while the case c) (see Section 5.6) corresponds to the case when Y is located after J and before B. The case d) (see Section 5.7) corresponds to the case when $Y = B$.

to the cycle σ_B, see Figure 7b. In this way we identified so far all elements of the cycle $\sigma_B = (E_1, \dots, E_d)$, with the exception of the label E_1.

5.3.2. *How to find the missing label* E_1*?* The information about the missing label E_1 is contained in one of the connected components of the two pruning procedures considered in Section 4.3 (more precisely, in the tree T which contains the black vertex B). Clearly, E_1 is the label on the edge which connects the vertex B to its parent in T. Regretfully, we do not have (yet) the access to this tree T. On the bright side, we do have the access to the outcome of the folding procedure (Section 4.3.3) applied to this tree T; the discussion from Section 4.3 shows that this outcome is just W (which is a white organic vertex) in the output tree T_2 as well as its all children, together with its parental edge. In the following we will describe how to reverse the folding procedure and, in this way, to recover the tree T (in the example from Section 4.3.3 it is the tree Figure 27a) from the outcome of folding (Figure 27b).

5.3.3. *The greedy algorithm.* Our first step is to identify the children $V_1, \dots, V_m$ (listed in the counterclockwise order) of the root of T; on the example from Figure 27a these vertices

$$V = (V_1, \dots, V_5) = (14, 18, 20, 21, 30) \tag{20}$$

are drawn in blue. In the following we will treat the aforementioned outcome of the folding as the list $L = (L_1, \dots, L_\ell)$ of the children of W in T_2, listed in the counterclockwise order. In the example from Figure 27b we have

$$L = (\mathbf{14}, 2, 11, \mathbf{18}, 8, 4, 6, 7, 10, 12, 3, 5, 9, \mathbf{20}, \mathbf{21}, 13, 16, \mathbf{30}, 15, 17); \tag{21}$$

with boldface we indicated the entries of V; on Figure 27b these boldface vertices are also drawn in blue.

Since the list L can be seen as an outcome of the depth-first search, it has the following structure:

$$\begin{aligned} L = \big(V_1, &\text{(the black descendants of } V_1), \\ &V_2, \text{(the black descendants of } V_2), \quad \dots, \\ &V_m, \text{(the black descendants of } V_m)\big). \end{aligned} \tag{22}$$

By Remark 4.1 each black descendant of V_i carries a label which smaller than V_i; furthermore $V = (V_1, \dots, V_m)$ is an increasing sequence. It follows that $V = (L_{i_1}, \dots, L_{i_m})$ is an increasing subsequence of L which can be found by the following *greedy algorithm*:

We set $i_1 = 1$ so that $V_1 := L_1$.

If i_k was already calculated, we define i_{k+1} as the smallest number $l \in \{i_k + 1, \dots, \ell\}$ with the property that $L_l > V_k = L_{i_k}$; we set $V_{k+1} := L_{i_{k+1}}$. If such a number l with such a property does not exist, the algorithm terminates.

In other words, we start with the empty list $V = \varnothing$ and read the list L. If the just read entry of L is greater than the last entry of V (or if V is empty), we append it to V. We leave it as an exercise to the Reader to verify that this greedy algorithm applied to L from (21) indeed gives (20).

5.3.4. *Recovering the black vertices in the tree T.* The above greedy algorithm identifies just the children of the root of T. In order recover the full structure of the tree T we use recursion, as follows. Equation (22) shows that the elements of the sequence V act like separators between the list of the black descendants of V_1, the list of the black descendants of $V_2, \dots$; in particular we are able to find explicitly such a list of the black descendants of any vertex V_i. In the example from (21) we have

$$\begin{aligned} &\text{(the descendants of } V_1 = 14) = (2, 11), \\ &\text{(the descendants of } V_2 = 18) = (8, 4, 6, 7, 10, 12, 3, 5, 9), \\ &\text{(the descendants of } V_3 = 20) = \varnothing, \\ &\text{(the descendants of } V_4 = 21) = (13, 16), \\ &\text{(the descendants of } V_5 = 30) = (15, 17). \end{aligned}$$

Each such a list of the descendants of V_i is again the outcome of the depth-first-search, this time restricted to the black descendants of the vertex V_i.

By applying the above greedy algorithm to the list of the descendants of the vertex V_i we identify the grandchildren of V_i, as well as the lists of the descendants of each of these grandchildren. For example, the greedy algorithm applied to the descendants of V_2

$$(\mathbf{8}, 4, 6, 7, \mathbf{10}, \mathbf{12}, 3, 5, 9)$$

shows that the vertex $V_2 = 18$ has three grandchildren: 8, 10, and 12, as well as gives the list of the descendants for each of them.

By applying the above procedure recursively, we recover the structure of the tree T (with the edge labels removed).

5.3.5. *Labels come back.* Our goal is to use the information about the outcome of the folding in order to recover the edge labels in the tree T.

Essentially, the above reconstruction of the tree T implies that we know which elementary folding operations from Figure 26 were performed. The only missing component in order to fully revert such an elementary folding operation at a black vertex b is the label of the edge f which connected b to its parent w in the tree T. We will denote by v the parent of b in the output tree T_2; the vertex v corresponds to the root of the folded version of T. Note that both w as well as v denote the parent of b; the difference lies in a different tree being considered. In fact, in order to solve the problem from Section 5.3.2 of finding the missing label E_1, we are interested in the special case when $b = B$ and $w = W$; with these notations $f = E_1$. Fortunately, before the folding was applied, the edge f and the edge g which connects w to its parent belonged to the same cluster, so they carried the same label. The problem is therefore reduced to finding explicitly the location of the edge g in the outcome of the folding.

Firstly, consider the generic case (shown on Figure 26) when the vertex w is not the root of the tree T. We denote by b_2 the black vertex which is the parent of w in T. In this case, after the folding at the vertex b_2 is performed, the label of the edge g will be stored in the edge connecting the vertex b_2 with its parent. This property will not be changed by further foldings of the tree T.

To summarize: in order to find the label f of the edge in the initial tree T_1 which connected the black vertex b to its parent w one should apply the following procedure. We apply the recursively the greedy algorithm from Section 5.3.4 to the children (in the output tree T_2) of the white vertex v which is the parent of b; this vertex v and its children correspond to the folded version of T. In this way we find the vertex b_2 which in the input tree T_1 is the grandparent of b. The desired label f is carried by the edge connecting b_2 with its parent v in the output tree T_2.

Consider now the exceptional case when the white vertex w is the root of the tree T. In fact, based on the information contained in the tree T_2 it is easy to check whether this exceptional case holds true by applying the greedy algorithm from Section 5.3.3 to the children of v and checking if the vertex b belongs to the list $(V_1, \dots, V_m)$.

In this case the edge h as well as its endpoints should be removed from Figure 26 since they do not belong to the tree T. The vertex w is attached to its parent by the parental edge g. This edge will not be modified by further steps of the algorithm; as a result our desired label f is stored in the folded version of T in the parental edge of the root, and hence in the output tree T_2 it is still stored in the edge g connecting $v = w$ with its parent.

5.4. **Cases (b), (c), (d):** $Y \neq J$**.** By Lemma 5.1, in these three cases W is an artificial white vertex thus the discussion from Section 4.4 and Figure 28 in particular are applicable here. We will study each of the cases (b), (c) and (d) in more detail in the following.

5.5. **Case (b): going counterclockwise around** W**, the vertex** Y **is after** B **and before** J**.** With the notations of Figure 28, our vertex B is one of the *blue neighbors* of w, located after j and before y (going counterclockwise around w), see Figure 28.

Since $B \neq Y$ it follows that we *did not* perform a jump operation of the form $\mathbb{J}_{\cdot,B}$, hence we performed a bend operation of the form $\mathbb{B}_{\cdot,B}$. As a consequence, the discussion from Section 5.3.1 is applicable also in our context; as a consequence we have found the labels $E_2, \dots, E_d$ which contribute to the cycle $\sigma_B = (\sigma_1, \dots, \sigma_d)$. As before, the remaining difficulty is to find the label E_1.

If we keep only the vertex w and the aforementioned blue neighbors of the vertex w, and declare that the edge between w and its parent j is the parental edge of the vertex w, we obtain a tree with w as a root. This tree T' is the outcome of the folding of the blue tree on Figures 8a and 9a. It follows that the algorithm from Sections 5.3.2 to 5.3.5 applied to T' gives the blue tree on Figures 8a and 9a and the desired edge E_1 can be recovered.

5.6. **Case (c): going counterclockwise around** W**, the vertex** Y **is after** J **and before** B**.** This case is fully analogous to the case b) considered in Section 5.5. The only difference is that instead of *blue* one should keep only the *red* neighbors of w, and one should take the edge connecting w with $y = Y$ as the parental edge of w.

5.7. **Case (d):** $B = Y$**.** In the case $B = Y$ we deduce that the vertex W was created by a jump operation of the form $\mathbb{J}_{\cdot,B}$.

5.7.1. *The labels* $E_2, \dots, E_d$. The following discussion is fully analogous to the one from Section 5.3.1. Proposition 3.2 and its proof imply that the black vertex B lost exactly two white neighbors from $\mathfrak{b}_J^{\text{initial}}$ when we performed the operation $\mathbb{J}_{\cdot,B}$ and never gained new ones. Using this information and Figures 8 and 9 we conclude that in the output tree T_2 the Stanley edge labels of the black vertex B all belong to cycle $\sigma_B = (E_1, \dots, E_d)$ (with the notations of Figures 8b and 9b these are the edges $E_3, \dots, E_d$).

The label of the edge E_2 is easy to recover: by Figures 8 and 9 we conclude that in the output tree T_2 the label E_2 is carried by the edge connecting W and J. The only remaining difficulty is to find the label E_1.

5.7.2. *How to find the missing label E_1?* The following discussion is somewhat analogous to the one from Sections 5.3.2 to 5.3.5.

With the notations from Figures 8 and 9 the missing label E_1 was also carried by the edge of the tree T_1 connecting v_1 with its parent x. This edge belongs also to the subtree T; regretfully we do not have (yet) access to this tree.

On the bright side, we do have the access to the outcome of the algorithm from Section 4.7.4. The organic children of J can be treated as separators which split the artificial children of J into a number of lists. Each such a list was generated by the depth-first search algorithm applied to the subtree attached to some organic child of J. The discussion from Section 5.3.3 is also applicable in our context with some minor modifications: the role of Remark 4.1 is played now by Remark 4.2, we now list the vertices in the *clockwise* order, and the greedy algorithm aims to find a *decreasing* subsequence. This, together with the analogue of Section 5.3.4 allows us to recover the structure of the tree T (without the edge labels yet).

In this way, using only the information contained in the tree T_2, we can find the vertex x which in the tree T was the grandparent of Y. There are the following two cases.

Firstly, if $x = J$ is the root of the tree T, the missing label E_1 is carried in the tree T_2 by the edge connecting J with its organic child W.

Secondly, if $x \neq J$ is not the root of T, the desired label E_1 appears in the pair (19) together with the vertex x. This means that the label of E_1 is carried by the first edge on the (very short) path which connects the vertex J with x in T_2.

5.8. **Recovering the cycles near the spine.** Our goal is to recover the cycle σ_B in the special case when B in the output tree T_2 is either a spine vertex or a neighbor of a white spine vertex. We will keep this assumption also in Sections 5.9 to 5.11.

In order to achieve this goal we need to recover the past of the white spine vertex (or the two white spine vertices) which is a neighbor of B.

5.8.1. *The fake symmetry.* From the discussion in Section 4.9 it follows that each white spine vertex of the output tree T_2 corresponds to some tree segment. At the first sight it might seem that the definition of a tree segment (or a backbone segment) has a *rotational symmetry* which corresponds to a rotation by 180° of Figures 30a and 30b and reversing the roles played by the sequences $A_1, \dots, A_r$ and $B_1, \dots, B_s$. This false impression may be reinforced by the apparent 180° symmetry of the output of the algorithm depicted on Figure 30c. In fact, this false symmetry of Figure 30c is problematic for our purposes because for a given white spine vertex W of the output tree T_2 we need to know which of its two black vertices plays the role of A_r and which one plays the role of B_s.

In order to resolve this ambiguity we split the set of neighbors of the white spine vertex W into two *halves*: each half consists of an endpoint of a spine edge and (going counterclockwise) the subsequent non-spine neighbors of W, up until the other spine neighbor, see Figure 30c. With these notations the set $\{A_1, B_1\}$ is equal to the set of two neighbors of W with the maximal labels in each of the halves respectively. The requirement that $A_1 < B_1$ gives us the unique way to fit Figure 30c into the the neighborhood of W.

5.8.2. *The first application of the greedy algorithm.* By applying the greedy algorithm from Section 5.3.3 we can reconstruct a large part of the information depicted on Figure 30b: recover the black vertices $A_1, \dots, A_r$ and $B_1, \dots, B_s$ as well as the folded versions of the trees $\alpha_1, \dots, \alpha_{r-1}, \beta_1, \dots, \beta_{s-1}, \gamma$.

Our prescription for finding the cycle σ_B will depend on the location of the black vertex on Figure 30b.

5.9. **Case (i): never-spine vertex.** Consider the case when B is a non-spine black vertex which is adjacent to a white spine vertex W and $B \notin \{A_1, \dots, A_r, B_1, \dots, B_s\}$; in other words B in the input tree T_1 was not a spine vertex. This means that B belongs to a folded version of one of the trees $\alpha_0, \dots, \alpha_{r-1}, \beta_1, \dots, \beta_{s-1}, \gamma$ (Figure 30b) and with the available information we can pinpoint this folded tree. The algorithm presented in Sections 5.3.1 to 5.3.5 is also applicable in this context. Note, however that this algorithm takes as an input a white vertex as a root surrounded by black vertices, *together with the parental edge of the root*, so we need to specify in each case this parental edge. For the tree α_i (with $i \in \{1, \dots, r-1\}$) it is the edge connecting W with A_{i+1}; for the tree β_i (with $i \in \{0, \dots, s-1\}$) it is the edge connecting W with B_{i+1}; for the tree γ it is the edge connecting W with B_1.

5.10. **Case (ii): post-spine vertices.** Consider the case when $B \in \{A_1, \dots, A_{r-1}, B_1, \dots, B_{s-1}\}$; in other words B was a black spine vertex in the tree T_1 but it is not a spine vertex in the tree T_2. It follows that the corresponding cycle can be written in the form $\sigma_B = (E_1, \dots, E_d)$, where E_1 and E_2 are the spine edges surrounding the vertex B, see Figure 30b. From the proof of Proposition 3.2 (Case 2) it follows that the vertex B lost two edges which are attracted to B, namely the two spine edges E_1 and E_2. In this way we recovered the edges $E_3, \dots, E_d$ (these are the edges which are attracted to B in T_2) and the remaining difficulty is to find E_1 and E_2.

The key observation is that all edges surrounding the vertex E_i (with $i \in \{0, \dots, r-1\}$) in the tree T_1 carried the same label; after performing the algorithm $\mathcal{A}$ this label is stored in the edge connecting W with A_{i+1}. Similarly, all edges surrounding the vertex F_i (with $i \in \{1, \dots, s-1\}$) in the tree T_1 carried the same label; after performing the algorithm $\mathcal{A}$ this label is stored in the edge connecting W with B_{i+1}. In this way we are able to recover the labels of all spine edges in the segment and, as a result, to recover the labels E_1 and E_2.

5.11. **Case (iii): spine vertices.** Consider now the case when B is a black spine vertex in the tree T_2. In the generic case when $B \notin \{1, n\}$ is not one of the endpoints of the spine, the vertex B lies on the interface between two tree segments. The cycle σ_B consists of: the edge labels lying on one side of the spine, followed by a single spine edge label, after which come the edge labels lying the other side of the spine, and the other spine edge label. From the proof of Proposition 3.2 (Case 2) it follows that the vertex B lost precisely these two spine edges; fortunately the discussion from Section 5.10 shows how to recover them.

6. Conclusion. Proof of Theorem 2.1

In Section 5 we constructed a map

$$\mathcal{A}^{-1} \colon \operatorname{Image}(\mathcal{A}) \to \mathcal{C}_{a_1,\dots,a_n}$$

which has the property that

$$\mathcal{A}^{-1} \circ \mathcal{A} = \operatorname{id} \colon \mathcal{C}_{a_1,\dots,a_n} \to \mathcal{C}_{a_1,\dots,a_n}$$

is the identity map. In particular, it follows that the map

$$\mathcal{A} \colon \mathcal{C}_{a_1,\dots,a_n} \to \mathcal{T}_{b_1,\dots,b_n}$$

is injective. It remains to show that it is also surjective.

A fast way to do this is to compare the cardinalities of the respective sets by Corollary 1.2 and (10). This proof has a minor disadvantage of being not sufficiently bijective.

An alternative but more challenging strategy is to notice that the map $\mathcal{A}^{-1}$ from Section 5 is well defined on $\mathcal{T}_{b_1,\dots,b_n}$. This time, however, one has to check that the image of $\mathcal{A}^{-1}$ on this larger domain is still subset of $\mathcal{C}_{a_1,\dots,a_n}$. The next step is to verify that

$$\mathcal{A} \circ \mathcal{A}^{-1} = \operatorname{id} \colon \mathcal{T}_{b_1,\dots,b_n} \to \mathcal{T}_{b_1,\dots,b_n}.$$

This method of proof does not create real difficulties, but it is somewhat lengthy. In order to keep this paper not excessively long we decided to omit this more bijective approach.

Acknowledgments

Research of the first named author was supported by Grant 2017/26/A/ST1/00189 of Narodowe Centrum Nauki. The second named author is grateful to Max Planck Institute for Mathematics in Bonn for its hospitality and financial support.

References

[Bia03] Philippe Biane. "Characters of symmetric groups and free cumulants". In: *Asymptotic combinatorics with applications to mathematical physics (St. Petersburg, 2001)*. Vol. 1815. Lecture Notes in Math. Springer, Berlin, 2003, pp. 185–200. DOI: `10.1007/3-540-44890-X\_8`.

[Bia96] Philippe Biane. "Minimal factorizations of a cycle and central multiplicative functions on the infinite symmetric group". In: *J. Combin. Theory Ser. A* 76.2 (1996), pp. 197–212. ISSN: 0097-3165. DOI: `10.1006/jcta.1996.0101`.

[Bia98] Philippe Biane. "Representations of symmetric groups and free probability". In: *Adv. Math.* 138.1 (1998), pp. 126–181. ISSN: 0001-8708. DOI: `10.1006/aima.1998.1745`.

[Cha09] Guillaume Chapuy. "A new combinatorial identity for unicellular maps, via a direct bijective approach". In: *21st International Conference on Formal Power Series and Algebraic Combinatorics (FPSAC 2009)*. Discrete Math. Theor. Comput. Sci. Proc., AK. Assoc. Discrete Math. Theor. Comput. Sci., Nancy, 2009, pp. 289–300.

[Dén59] József Dénes. "The representation of a permutation as the product of a minimal number of transpositions, and its connection with the theory of graphs". In: *Magyar Tud. Akad. Mat. Kutató Int. Közl.* 4 (1959), pp. 63–71. ISSN: 0541-9514.

[DFŚ10] Maciej Dołęga, Valentin Féray, and Piotr Śniady. "Explicit combinatorial interpretation of Kerov character polynomials as numbers of permutation factorizations". In: *Adv. Math.* 225.1 (2010), pp. 81–120. ISSN: 0001-8708. DOI: `10.1016/j.aim.2010.02.011`.

[Fér09] Valentin Féray. "Combinatorial interpretation and positivity of Kerov's character polynomials". In: *J. Algebraic Combin.* 29.4 (2009), pp. 473–507. ISSN: 0925-9899. DOI: `10.1007/s10801-008-0147-y`.

[Fér10] Valentin Féray. "Stanley's formula for characters of the symmetric group". In: *Ann. Comb.* 13.4 (2010), pp. 453–461. ISSN: 0218-0006. DOI: `10.1007/s00026-009-0038-5`.

[GR07] I. P. Goulden and A. Rattan. "An explicit form for Kerov's character polynomials". In: *Trans. Amer. Math. Soc.* 359.8 (2007), pp. 3669–3685. ISSN: 0002-9947. DOI: `10.1090/S0002-9947-07-04311-5`.

[IK99] V. Ivanov and S. Kerov. "The algebra of conjugacy classes in symmetric groups, and partial permutations". In: *Zap. Nauchn. Sem. S.-Peterburg. Otdel. Mat. Inst. Steklov. (POMI)* 256.Teor. Predst. Din. Sist. Komb. i Algoritm. Metody. 3 (1999), pp. 95–120, 265. ISSN: 0373-2703. DOI: `10.1023/A:1012473607966`.

[Las08] Michel Lassalle. "Two positivity conjectures for Kerov polynomials". In: *Adv. in Appl. Math.* 41.3 (2008), pp. 407–422. ISSN: 0196-8858. DOI: `10.1016/j.aam.2008.01.001`.

[Rat08] A. Rattan. “Stanley’s character polynomials and coloured factorisations in the symmetric group”. In: *J. Combin. Theory Ser. A* 115.4 (2008), pp. 535–546. ISSN: 0097-3165. DOI: 10.1016/j.jcta.2007.06.008.

[Śni13] Piotr Śniady. “Combinatorics of asymptotic representation theory”. In: *European Congress of Mathematics*. Eur. Math. Soc., Zürich, 2013, pp. 531–545.

[Śni16] Piotr Śniady. “Stanley character polynomials”. In: *The mathematical legacy of Richard P. Stanley*. Amer. Math. Soc., Providence, RI, 2016, pp. 323–334. DOI: 10.1090//mbk/100/19.

[Sta03] Richard P. Stanley. “Irreducible symmetric group characters of rectangular shape”. In: *Sém. Lothar. Combin.* 50 (2003/04), Art. B50d, 11.

[Sta06] Richard P. Stanley. *A conjectured combinatorial interpretation of the normalized irreducible character values of the symmetric group*. 2006. arXiv: arXiv : math/0606467v2 [math.CO].

[Woj21] Karolina Wojtyniak. “Bijection between trees in Stanley character formula and factorizations of a cycle”. In: *Sém. Lothar. Combin.* 85B (2021), Art. 25, 12.

Email address: karolina5284@wp.pl

MAX-PLANCK-INSTITUT FÜR MATHEMATIK - BONN, VIVATSGASSE 7, 53111 BONN, GERMANY
Email address: psniady@impan.pl